RSC Advances

ROYAL SOCIETY OF CHEMISTRY

www.rsc.org/advances

The role of SBA-15 in drug delivery

Vaezeh Fathi Vavsari[a], Ghodsi Mohammadi Ziarani[a*], Alireza Badiei[b]

[a] *Department of Chemistry, Alzahra University, Vanak Square, P.O. Box 1993893973, Tehran, Iran*

[b] *School of Chemistry, College of Science, University of Tehran, 14155-6455, Tehran, Iran*

**Corresponding author Email address: gmziarani@hotmail.com, gmohammadi@alzahra.ac.ir*

Received (in XXX, XXX) Xth XXXXXXXXX 20XX, Accepted Xth XXXXXXXXX 20XX
DOI: 10.1039/b000000x]

Abstract

Controlled drug-delivery systems (DDSs) are one of the ideal methods for human health care in which the drug is released with a constant rate and its concentration in blood remains always steady. Pure and modified SBA-15, with a hexagonal structure and nano size pores has apiary-like structure, have attracted much attention as carriers in academic researches for delivery of natural and chemical drugs. In this review, preparation, characterization and application of various types of SBA-15 as drug delivers is investigated.

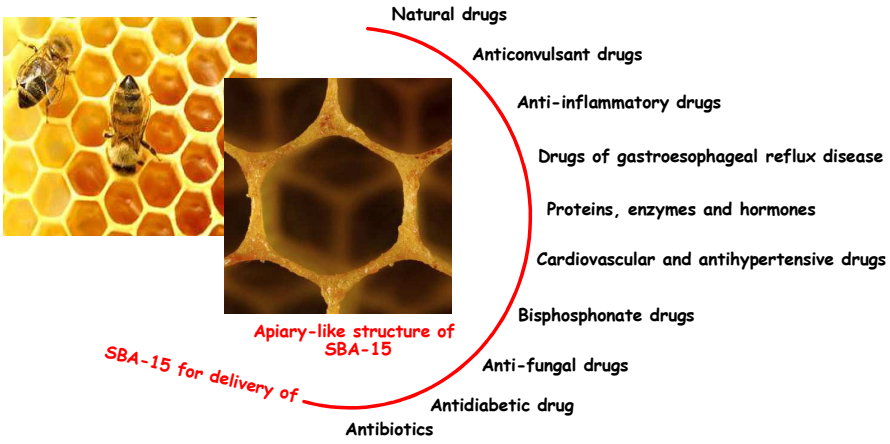

Keywords: SBA-15, Drug delivery, Drug release, Mesoporous materials, Nanomedicine

Contents

Abbreviations

AAMs	Anodic Alumina Membranes	**PAA**	Poly(Acrylic Acid)
AIE	Aggregation-induced Emission	**PD**	Poly(Diallyldimethylammonium Chloride)
APMS	Aminopropyldimethoxymethylsilane	**PDDA**	Poly(Dimethyldiallylammonium Chloride)
APTMS	3-Aminopropyltrimethoxysilane	**PEI**	Poly(Ethyleneimine)
BET	Brunauer–Emmett–Teller	**PL**	Photoluminescence
BSA	Bovine Serum Albumin	**PLGA**	Polymer of Lactic-co-glycolic Acid
CNT	Carbon Nanotubes	**PMO**	Periodic Mesoporous Organosilica
DAB	Diaminobutane	**PNIPAAm**	Poly(*N*-isopropylacrylamide)
DDSs	Drug-delivery Systems	**Pr**	Propyl
FaSSIF	Fasted State Simulated Intestinal Fluid	**PS**	Post-synthesis
HC	Hydroxypropyl Cellulose	**PSS**	Poly(Sodium4-styrenesulfonate)
HC	Hydrocortisone	**SBA-15**	Santa Barbara Amorphous
HPLC	High-performance Liquid Chromatography	**SBF**	Serum Blocking Factor
HPMCP	Hydroxypropyl Methylcellulose Phthalate	**SC**	Supercritical
LCST	Lower Critical Solution Temperature	**SCK**	SiO_2-CaO-K_2O
LDH	Layered Double Hydroxide	**SEM**	Scanning Electron Microscope
MC	Mesoporous Carbon	**SGF**	Sarcoma Growth Factor
MCM-48	Mobil Crystalline Materials	**TEOS**	Tetraethylorthosilicate
MH	Metformin Hydrochloride	**TGA**	Thermogravimetric Analysis
MP	Methylprednisolone	**TREN**	Tris(2-aminoethyl)amine
MPSn	Methylphenyltin	**TSDAE**	Triethoxysilanylundecanoic Acid Ethyl Ether
MPTS	3-Mercaptopropyltrimethoxysilane	**TUD-1**	Technische Universiteit Delft
NSAIDs	Nonsteroidal Anti-inflammatory Drugs	**UO**	Urate Oxidase
OPS	One-pot Synthesis	**UV-Vis**	Ultraviolet-Visible
OTMS	Octyltrimethoxysilane	**β-CD**	β-Cyclodextrin

1. Introduction

The history of drug therapy went back to many years ago when human began to use natural medicine specially plants for treatment of diseases. To date, various natural and chemical medicines have been produced as oral ingestion or intravascular injection. In traditional medicine the drug is distributed throughout the body by the systemic blood circulation and only a small portion of the drug reaches the organ. Moreover, the drug is released burstly and its concentration changes through the blood in a period of time. Controlled drug-delivery systems (DDSs) are one of the ideal methods for human health care in which the drug is released with a constant rate and its concentration in blood remains always steady.[1, 2]

Since the discovery of mesoporous silica M41S in 1992[3], a rapid growth has been appeared in research and development of the mesoporous materials. In this regards, mesoporous silica materials have attracted much attention as carriers for delivery of various drugs because of their high specific surface area, ordered structure, and large pore volume. There are many review articles about the synthesis and application of various types of mesoporous carriers in the delivery of drug.[4-8] Santa Barbara Amorphous (SBA-15) which was synthesized for the first time in 1998 by Zhao and coworkers,[9, 10] is a kind of mesoporous silica with a hexagonal structure, large pore size, high surface area, great pore wall thickness, and high thermal stability. Following our previous publications,[11, 12] here, we want to review the role of SBA-15 and the modified SBA-15 by the use of organic and inorganic compounds on drug delivery processes. Moreover, comparison of the drug adsorption and release ability of the modified and unmodified SBA-15 is another aim of this article. As shown in Chart 1, the use of SBA-15 in drug delivery publications attracted many attentions in recent years.

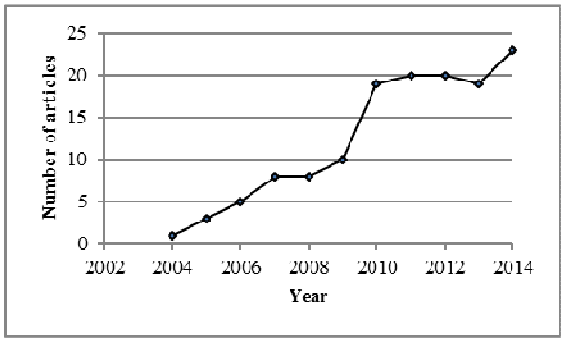

Chart 1: Progress of the SBA-15 application in drug delivery since 2004 (the data analysis was performed by Scopus)

2. Preparation and surface analysis of SBA-15

Pure silica SBA-15 can be synthesized according to the method described by Zhao and coworkers, in which, tri-block copolymer Pluronic P123 (3.0 g) was dissolved in water (30 g) and HCl solution (120 g, 2 M) with stirring at 35 °C. Then, tetraethylorthosilicate (TEOS, 8.50 g) was added into that solution with stirring at 35 °C for 20 h. Following, the mixture was aged at 80 °C overnight without stirring. After this time, the solid product was recovered, washed, and air-dried at room temperature with the yield of about 98% (based on silicon). Calcination was carried out by gradual increase in temperature from room temperature to 500 °C in 8 h and it was continued at 500 °C for 6 h to remove the surfactant and obtain a hollow mesoporous compound.[10]

2.1. Functionalization of SBA-15 with organic and inorganic materials

There are two methods for functionalization of SBA-15 including the direct synthesis or co-condensation, and the post-synthesis or grafting. In co-condensation method, organic and inorganic compound is added to the mixture of SBA-15 precursors and the final product has the material (organic and/or inorganic) in its matrix. In grafting of the organic compounds, organosilanes $RSi(OR')_3$, silazanes $HN(SiR_3)_2$ and/or chlorosilanes $ClSiR_3$ react with free silanol groups on the SBA-15 surface. However, in co-condensation process, *tetra*alkoxysilanes $(RO)_4Si$ reacts with terminal *tri*alkoxyorganosilanes $(R'O)_3SiR$.[12]

2.2. *In vitro* stability of SBA-15 under physiological conditions

The numerous applications of SBA-15 as carrier are highly dependent on its stability in the implied conditions. Izquierdo-Barba and coworkers investigated the stability of pure and modified SBA-15 in aqueous solutions mimicking physiological fluids at 37 °C. The selected solutions were saline solution, simulated body fluid and completed Dubecco's modified Eagle medium which are widely used as release media in drug delivery. The obtained results indicated that the pure SBA-15 degraded in all solutions and it had a partial loss of the mesostructure after 60 days of the assay. In addition, the modified samples were more stable than pure SBA-15 due to the organic functional

groups; they protect the siloxanes of the silica structure against the nucleophilic addition of water that leads to the preservation of the mesostructure arrangement.[13]

3. The role of pure and modified SBA-15 in adsorption and release of drugs

3.1. Natural drugs (herbal medicine)

3.1.1. Salvianolic acid B

Rhodamine B (RhB) is a highly fluorescent dye used as a tracer. It is covalently grafted towards the mesoporous channels of SBA-15 using co-condensation method and resulted in placement of positive charges on the pore surface of SBA-15 as well as red fluorescent emission. Then, negatively charged salvianolic acid B (SAB) ions were loaded into the pores of SBA/RhB to construct a drug delivery system (Scheme 1). SAB is a major water-soluble polyphenolic acid that eliminates reactive oxygen species and inhibits hepatic fibrosis. The blood compatibility of the carrier SBA/RhB-SAB was evaluated using investigation of the hemolysis and coagulation behaviors in a broad concentration range (50-500 mg/ml) under *in vitro* conditions. The results showed that SBA/RhB-SAB possessed good blood compatibility.[14] SAB is isolated from *Salvia miltiorrhiza* which widely used for the treatment of cardiovascular and cerebrovascular diseases.[15]

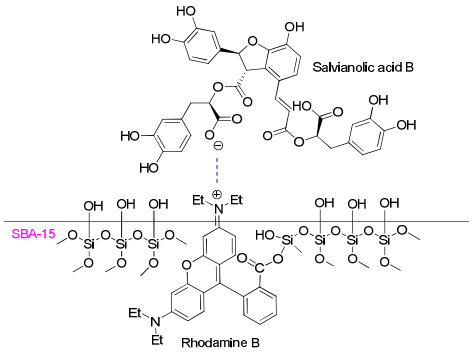

Scheme 1: The pore structure of SBA/RhB-SAB

3.1.2. Baicalin

Baicalin (BC) is a type of bioactive flavonoid found in Chinese medicinal herb Huang-chin. There are many hydroxyl groups in the baicalin structure as shown in Scheme 2

that may serve as proton donors to form hydrogen bonds with the surface of carriers. Therefore, SBA-15 is a good candidate for it as a carrier because of the large pore size and the presence of silanol groups on its surface. Two types of SBA-15 were used for this aim, including the pure SBA-15 and SBA-15-Pr-NH_2. TGA analysis showed that the total mass storage of BC onto the SBA-15 and SBA-15-Pr-NH_2 was 36.3 and 39.1 weight%, respectively. The released amount of BC represented 15.2% from BC/SBA-15 in 72 h while it was 98.4% for BC/SBA-15-Pr-NH_2 at the same time. This confirms that the modification of SBA-15 surface with amino groups increases the delivery rate of the BC from mesoporous material as the hydrogen bonds between SBA-15 surface and BC decrease. In addition, basic aminopropyl groups would accelerate the adsorption of acidic BC in the mesoporous channels.[16]

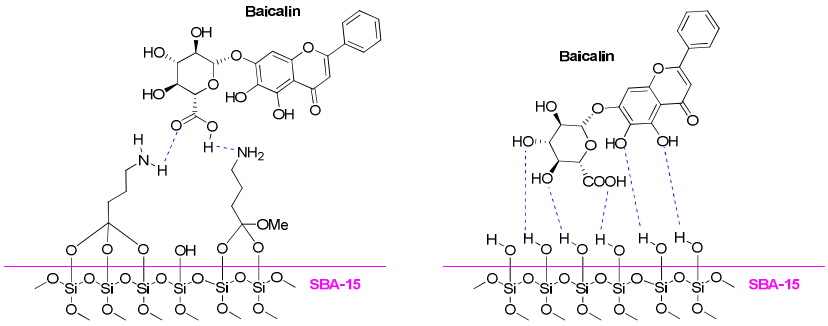

Scheme 2: differences between interaction of BC with surface of SBA-15 and SBA-15-Pr-NH_2

3.2. Nonsteroidal anti-inflammatory drugs (NSAIDs)

3.2.1. Ibuprofen

Ibuprofen (IBU) is a NSAIDs drug to relieve pain and treatment of fever. In recent years, it attracted attention of investigators for drug delivery abilities of mesoporous materials, especially SBA-15, because of its molecular size at a range of 0.6-1 nm which is suitable to load into the nano-size pores of these materials. Germany researchers loaded IBU into the SAB-15 pores by dissolving IBU in ethanol or hexane, and then adding activated SBA-15 to it at room temperature; after 12 h, SBA-15/IBU was extracted. It showed that the mobility of the molecules located more in the center of the pores, on the one hand, and the slow dynamics of the molecules adsorbed on the pore walls, on the other hand, can be advantageously used to tune the release of the drug

to achieve a desired kinetic profile.[17-19] The influence of mesoporous structure (3D-bicontinuous cubic MCM-48 and 2D-hexagonal SBA-15) on the controlled delivery of IBU has been published and demonstrated that the structure characteristics cannot affect the release kinetic profiles of IBU. Surface functionalization of SBA-15 with hydrophobic octadecyl chains making it work faster delivery system than simple SBA-15 because of the decreasing interaction of IBU with the surface.[20] Heikkilä *et al.* proved that SBA-15 reaching a very high IBU load of 1:1 in weight due to its high pore volume in comparison with MCM-41 and TUD-1.[21]

Functionalization of SBA-15 with amine groups using 3-aminopropyltrimethoxysilane (APTMS) through one-pot synthesis (OPS) and postsynthesis (PS) gave SBA-15-Pr-NH_2 as a matrix for controlled drug delivery. IBU and bovine serum albumin (BSA) were selected as model drugs and loaded onto the pores of SBA-15 and SBA-15-Pr-NH_2, finally, the results were compared. As shown in Table 1, the surface area, pore size and pore volume of PS-SBA-15-NH_2 is lower than the corresponding OPS type; it proves that grafting of the amino groups on the internal surface of pure SBA-15 (PS) has occurred, with the reduction of surface areas as well. Amounts of IBU loading for PS types are more than OPS, whereas, the results for BSA are very lower than OPS since the smaller pores of PS-SBA-15-Pr-NH_2 against large protein molecules as BSA. OPS-SBA-15 is a better composite than PS-SBA-15 as protein delivers matrix, because not only it can adsorb a large amounts of BSA, but also provide a favorable hydrophilic surface which can better preserve the coherent structures and native states of proteins. The release rate of IBU/PS-SBA-15 is found to be effectively controlled as compared with IBU/pure SBA-15 and IBU/OPS-SBA-15 to the ionic interaction between carboxyl groups in IBU and amine groups.[22] The study of the pH-dependence IBU release from PS-SBA-Pr-NH_2 demonstrated that it was slower at pH=2 (~pH of stomach body) and faster at pH=4 (~pH of proximal intestine), however, more than 80% of IBU was released in 5 h at pH=7.[23] Szegedi and co-workers proved that amino modification of surface resulted in a high degree of IBU loading and slow rate of release for MCM-41, whereas it was completely different for SBA-15.[24] SBA-15 was also modified with 3-(2-aminoethylamin)propyltrimethoxysilane to give SBA-Pr-NH-(CH_2)-NH_2 as ibuprofen carriers for study the influence of mesoporous structure on drug delivery

property. The maximum loaded IBU onto SBA-Pr-NH-(CH_2)-NH_2 was 20 mg/0.1 g, however, it showed the initial burst release (60 weight%) before 3 h.[25]

Table 1: The characteristics comparison of various functionalized SBA-15 and their abilities in drug loading[22]

Sample name	APTES/TEOS[1] (mol %)	APTES/SBA-15 (mmol/g)	BET[4] surface area (m^2/g)	Pore size (Å)	Pore Vol (cm^3/g)	Loading amount of IBU (wt %)	Loading amt of BSA (wt %) at pH 4.7
OPS0[2]	0	-	602	86	0.96	14.6	9.9
OPS1	4	-	571	86	0.93	16.9	28.5
OPS2	5	-	590	86	0.95	23.8	34.2
OPS3	6	-	570	-	0.73	17.5	30.1
PS0[3]	-	0	860	86	1.20	25.6	8.1
PS1	-	8	473	78	0.76	20.6	1.1
PS2	-	16	458	78	0.70	29.9	1.5
PS3	-	24	469	78	0.75	37.2	2.2

[1]Tetraethylorthosilicate
[2]One-pot synthesis
[3]Postsynthesis
[4]Brunauer–Emmett–Teller technique

Lee *et al.* demonstrated that SBA-15 functionalized with amine and/or diamine has the more IBU loading capacity than SBA-15-Pr-SO_3H. Moreover, the IBU release rate of SBA-15-Pr-SO_3H is faster than the others.[26] Tetraphenylethen is an aggregation-induced emission luminogen (AIE) compound which was grafted onto the SBA-15-Pr-NH_2 pores. The material emitted blue light upon UV irradiation. After loading of the IBU drug into the pores of SBA/AIE (Scheme 3), the fluorescence intensity of the material is further enhanced and was photostable for the drug loading and release process, indicating its great potential for biomedical applications.[27]

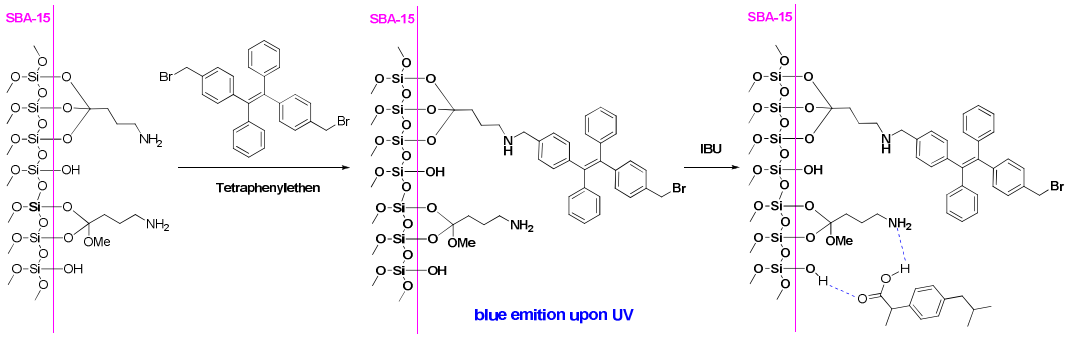

Scheme 3: the structure of SBA/AIE-IBU

In another publication, SBA-15-Pr-NH_2 reacted with glutaraldehyde to give a bridged functionalized SBA-15 as shown in Scheme 4. The surface area of this hydrophobic

bridged-SBA was decreased from 802 to 62 m^2g^{-1} and pore diameter from 8.0 to 6.0 nm, which ultimately increased drug loading capacity from 18.0 up to 28.3% and resulted in a very slow release rate of IBU over the period of 72.5 h.[28]

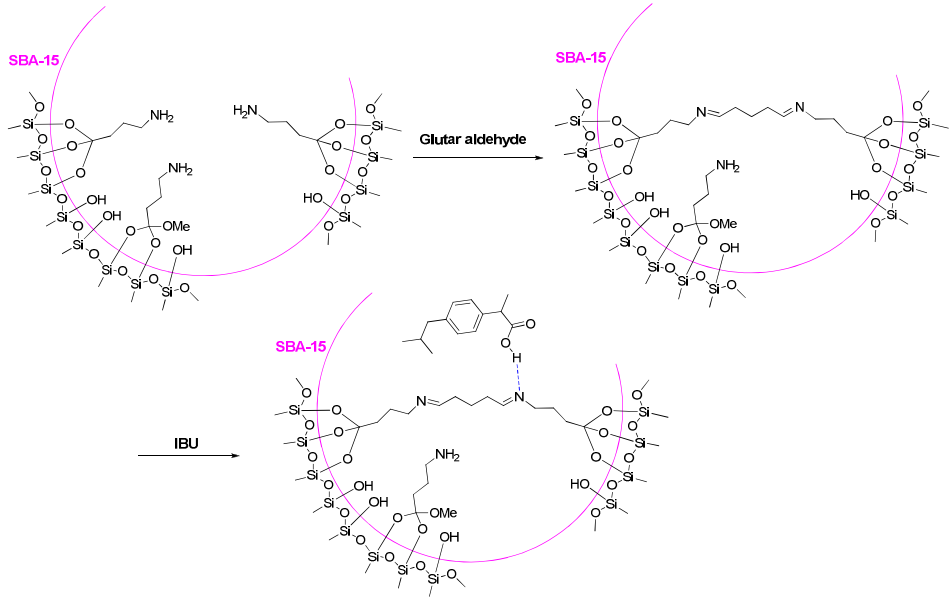

Scheme 4: the structure of SBA-15-Pr-NH_2 bridged by glutaraldeyde

Tian and Yang synthesized a thermosensitive nano-composite of SBA-15/poly(*N*-isopropylacrylamide) (PNIPAAm) *via* in situ radical polymerization of the mesopore. Then, they used the nano-composite as carrier to construct temperature-responsive controlled IBU delivery system (Scheme 5). The results showed that the loading level of IBU can be regulated by polymer content in pores using interaction between IBU and polymer and trap effect of the polymer chains in pores. Also, the material was reversible fast/slow transitions switches or rate regulator responsive by changing temperature around the lower critical solution temperature (LCST) and to be potentially interesting in smart controlled delivery.[29]

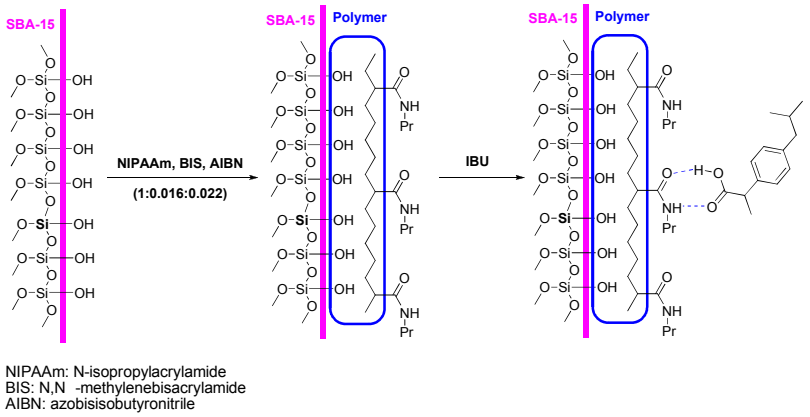

Scheme 5: the structure of SBA-15/PNIPAAm-IBu

Some types of tailored made SBA-15 were designed using the three generations of synthesized diaminobutane (Scheme 6) based poly(propyleneimine) dendrimers ($DAB(NH_2)_x$). The alkoxysilane groups were grafted on the surface of SBA-15 pores, separately, (Scheme 7) to give organic-inorganic hybrid materials $DAB(NH_2)_x$/SBA. To evaluate the potential application of these hybrids as controlled delivery systems, IBU was selected as a model drug for adsorption and *in vitro* release assays were accomplished. The results revealed that the higher dendrimer generation of composite, increases the host–guest attracting interactions and, consequently increases the IBU loads. As shown in Table 2 (based on the Higuchi model),[30] with regression factors >0.99, the linear interval varies from 10 hours for the released IBU from SBA-15 to 22-34 hours for $DAB(NH_2)_x$/SBA with G1-G3 dendrimers. Also, the *k* values progressively increase when ranging from pure SBA-15 to $DAB(NH_2)_x$/SBA with G1-G3 dendrimers. This is especially important to minimize the risks of overdoses when the local administration of certain pharmaceuticals is aimed.[31]

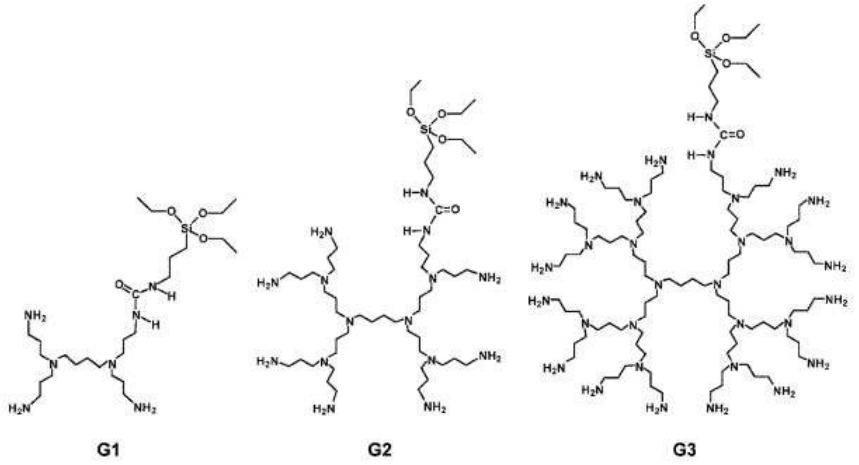

Scheme 6: Schematic representation of dendritic precursor G1-G3

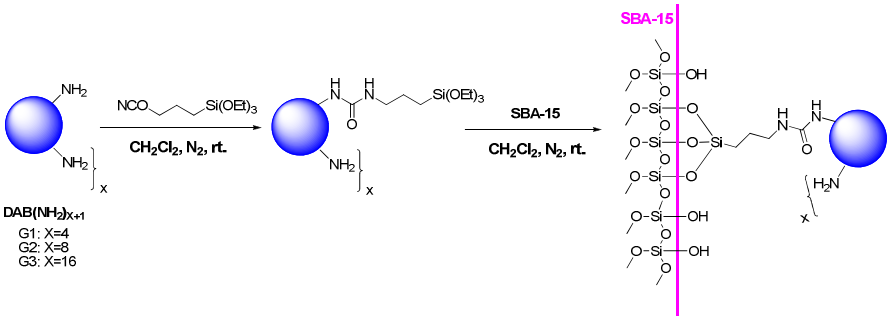

Scheme 7: Functionalization of SBA-15 with dendritic amines

Table 2: Ibuprofen adsorption and release data from different mesoporous samples[31]

Sample	[IBU] loaded (mg/g SiO_2)	k (mg g^{-1} $h^{1/2}$) [IBU]=$k.t^{1/2}$	Regression factor	Linear interval [IBU] *vs.* $t^{1/2}$ (h)
SBA-15	215	40.0 ± 3.4	0.990	0-10
SBA-15-G1	288	53.7 ± 0.6	0.999	0-22
SBA-15-G2	408	66.7 ± 2.1	0.997	0-27
SBA-15-G3	480	73.9 ± 4.1	0.990	0-34

Submicron particles of MgO/SBA-15 were synthesized by a simple one-pot synthesis approach and used as an IBU carrier for controlled release. Due to the alkalinity of MgO species on the surface, the more amount of IBU adsorbed on the surface of MgO/SBA-15 than the pure SBA-15, although the surface area was decreased by the surface

modification. In the first 6 h of the *in vitro* test of IBU release , only 63% of the adsorbed IBU was released from the MgO/SBA-15 (Si/Mg=20).[32]

Cauda *et al.* synthesized a type of SBA-15, a macroporous bioactive glass–ceramic scaffold (SiO_2-CaO-K_2O: SCK), as a local drug delivery composite for tissue engineering. The uploaded IBU onto the SBA-15-SCK was 11.5% wt, and the release of IBU from the SBA-15-SCK composite was approximately 40% w/w after 10 h, while IBU was completely released from IBU/SBA-15 after this time.[33]

Magnetic SBA-15 composites were synthesized using separately the addition of three different types of SBA-15 into a solution of CH_3COOH/HNO_3 and $Fe(acac)_3$ (iron (III) acetylacetonate), after 4 hours, the materials were collected and calcined at 500 °C. The three types of resulting Fe_xO_y/SBA-15 were then suspended in a solution of IBU in n-hexane for 48 h. The loading degree of the drug into the pores of composites was determined by TGA (22-29% wt). In addition, drug releasing of the IBU/composites in simulated body fluids were in a range of 11-22% wt within 2 hours. These composites (Scheme 8) showed a magnetic response sufficient for drug targeting in the presence of an external magnetic field (Fig. 1).[34]

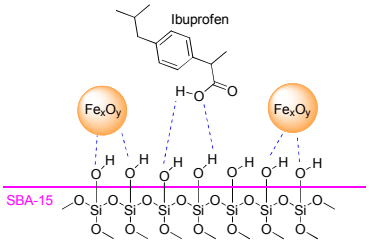

Scheme 8: The structure of IBU-Fe_xO_y/SBA-15

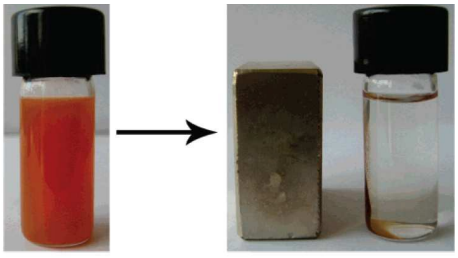

Fig. 1: The composite of IBU-Fe_xO_y/SBA-15 in the absence and presence of magnetic field[34]

Another type of magnetic SBA-15 was prepared by Zhu and coworkers which was formed from $Fe(CO)_5$ *via* the surfactant-template sol-gel method and control of transport through polymerization of *N*-isopropylacrylamide inside the pores. Hydrophobic $Fe(CO)_5$ not only acted as a swelling agent, but also, it played the role of magnetic particles. The obtained PNIPAAm-$Fe(CO)_5$/SBA-15, with the pore size and pore volume of 7.1 nm and 0.41 cm^3g^{-1}, respectively, has high drug storage capacity. It was a successful controlled delivery system for IBU, which release exhibited a pronounced transition at around 32 °C.[35] In another publication of Zhu team, they used $FeCl_2$ instead of $Fe(CO)_5$ during the synthesis of magnetic SBA-15 and with the use of calcinations technique, Fe_3O_4/SBA-15 was obtained. After polymerization, it had pore diameter 3.8 nm and pore volume 0.47 cm^3g^{-1} which is close to the properties of PNIPAAm-$Fe(CO)_5$/SBA-15. PNIPAAm-Fe_3O_4/SBA-15 was also an active IBU releasing system around 17 °C indicating a typical thermo-sensitive release property for it.[36]

Chinese researchers designed γ-Fe_2O_3-SBA-15 [37] and also PLGA-magnetic SBA-15 [38] using $Fe(NO_3)_3.9H_2O$ for IBU delivery. PLGA is a polymer of lactic-co-glycolic acid. The system showed a good pH-dependent drug releasing in which PLGA inhibited the release of IBU in pH=7.4 whereas dissolution of PLGA in a media with pH=1.2 led to IBU releasing from the carrier. Meanwhile, the magnetic γ-Fe_2O_3 nanoparticles onto the pores of PLGA-IBU-magnetic SBA-15 make it conductible using an external magnetic field and potential hyperthermia.[38]

Luminescence $YVO_4:Eu^{3+}$ phosphor layer was subjected onto the SBA-15 using the Pechini sol-gel process,[39] resulting in the formation of the $YVO_4:Eu^{3+}$/SBA-15 composite material with the strong red luminescence (Fig. 2). This composite may be a perfect drug delivery system because of its photoluminescence property, so IBU was used as a model drug. In comparison with the IBU-SBA-15, it showed only slightly lower IBU storage capacity, although, exhibited strong red luminescence even after IBU loading. In addition, during the release of the IBU, the PL intensity increased and reached to maximum when IBU was completely released from the system.[40] These properties make it easily identifiable, trackable and monitorable by the change of luminescence during drug delivery.

Fig. 2: Functionalized SBA-15 with $YVO_4:Eu^{3+}$, Left: Schematic Functionalized SBA-15, Middle: $YVO_4:Eu^{3+}$/SBA-15 under the Irradiation of a 365 nm UV Lamp in the Dark, Right: TEM image of $YVO_4:Eu^{3+}$/SBA-15.[40]

Silicon nanocrystal (ncSi) is one of the photoluminescence materials which is grafted into the structure of SBA-15 and led to the production of a fluorescence mesoporous material (ncSi/SBA-15) (Fig. 3, left). It was tested as a carrier for delivery of IBU. The loading amount of IBU determined in it and was 299.29 mg/g which is a little less than un-modified SBA-15 (301.46 mg/g). The drug release of IBU-ncSi/SBA-15 was similar to the IBU/SBA-15. Also, it showed opportunities for light-emitting labels (Fig. 3, right), biomedical imaging and targeted drug delivery.[41] Another type of Si-SBA-15 was synthesized using magnesiothermic reduction of SBA-15. The resulted mesoporous semiconductor silicon possesses unique mesopores itself. Release profile of IBU/Si-SBA-15 exhibited that 40 wt% IBU was released within 2 h, more than 80 wt% was released over the period of 20 h. In comparison with SBA-15, it could be observed that the IBU release from Si-SBA-15 is slower than SBA-15. IBU, a hydrophobic drug, could have stronger interaction with silicon than silica.[42]

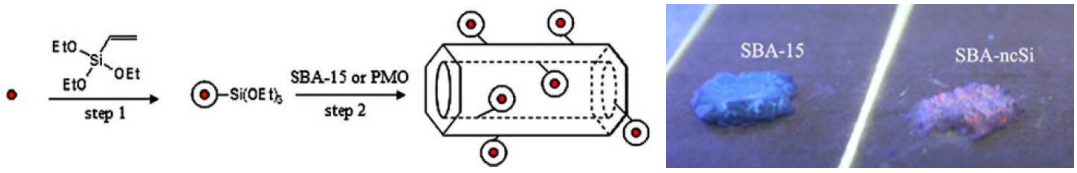

Fig. 3: SBA-15/ncSi, Left: the synthesis method and final structure system, Right: photoluminescence differences of SBA-15 and SBA-15/ncSi under UV irradiation.[41]

3.2.2. Ketoprofen

SBA-15-Pr-NH_2 was used as carrier for ketoprofen (KET, an anti-inflammatory drug). The maximum uptake of KET in pure SBA-15 and SBA-15-Pr-NH_2 was 7 and 18 wt%, respectively. The release profile was investigated in different pH (1.2, 4.5 and 8.4). KET/SBA-15-Pr-NH_2 was slower than KET/SBA-15 in all cases and acidic solution (pH 1.2) showed the best pharmaceutical availability.[43]

3.2.3. Naproxen

Naproxen (NPX) is commonly used for relief of a wide variety of pain, fever, swelling and stiffness.[44] It was loaded into the pores of SBA-15 and SBA-15-Pr-NH_2. The loaded amount of NPX into unmodified and amine-modified SBA-15 was similar. The released rate of NPX/SBA-15 was faster than NPX/SBA-15-Pr-NH_2 which represented 90.7% and 80.9% release in 72 h, respectively.[45]

3.2.4. Aspirin and salicylic acid

Magnetic Fe_3O_4/SBA-15 was filled with aspirin (ASP) molecules up to 13 wt%. The release behavior of aspirin from ASP-Fe_3O_4/SBA-15 was investigated in SBF which showed a relatively slow release rate (70% in 48 h).[46] Furthermore, Rosenholm and Lindén investigated pH-dependent of salicylic acid adsorption on the amino modified surface of SBA-15.[47]

3.2.5. Indomethacin

Stability of high indomethacin (IND) content formulations based on MCM-41 and SBA-15 materials was studied before and after 3 month storage in stressed conditions. After this time, the physical stability of the IND/MCM-41 and IND/SBA-15 was found acceptable and the IND release was rapid, but some impairment was observed in the chemical stability. A decrease in the loading degree and IND degradation product formation were observed, especially in MCM-41 based samples after stressing.[48] Also, IND/SBA-15 showed the best physical stability and biocompatibility in comparison to other mesoporous materials.[49]

3.3. Vasodilators

3.3.1. Papaverine

Papverine (PAP) is an opium alkaloid, used primarily in the treatment of various spasms. SBA-15 was used as a carrier for PAP in three different forms of granulation, coating with stearic acid (SA) and tablet preparation using hydroxypropyl cellulose (HC). An addition of SA and HC as modifiers allowed to extend the PAP release. The release rate for samples was PAP/SBA > SA-PAP/SBA > HC-PAP/SBA, thus, the best kinetics of PAP release and the highest pharmaceutical availability were achieved from HC-PAP/SBA-15. This behavior induced by difficult diffusion of the PAP molecules through the layer of forming hydrogel from hydrophilic polymer. Retardation of release process may result from slower penetration of water inside the pores of SBA-15 due to the polymer layer formation.[50] In another publication, SBA-Pr-SO_3H was used as carrier for PAP. The maximum amount of adsorbed PAP was about 16 wt% and showed the slow release from the composite in which after 48 h cumulative releases does not cross 80%.[51]

3.4. Psychoactive drugs

3.4.1. Caffeine

An *in situ*, one-step encapsulation of caffeine (CAF) onto SBA-15 was accomplished by Liédana and co-workers. Then, the *in situ* synthesized CAF/SBA-15 was compared to the adsorbed CAF in SBA-15 (ad-CAF/SBA-15). CAF/SBA-15 and ad-CAF/SBA-15 showed 23 and 15.8 wt% CAF encapsulated. The existence of miracles and surrounding silica with van der Waals and hydrogen bonds interactions with CAF (Fig. 4), respectively, leads to enhancement of CAF encapsulation by *in situ* procedure. Nevertheless, the micelles were not an efficient barrier to the release of caffeine; micelled CAF were quickly released from CAF/SBA-15, while the complete release of the CAF molecules occurred in about half a day due to adsorption on the pore wall silica. Also CAF/SBA-15 showed higher loading than CAF/silica type.[52]

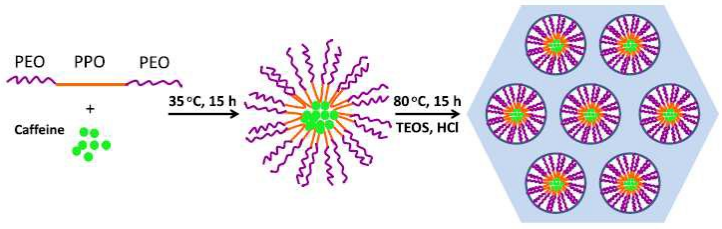

Fig. 4: Micelled encapsulation of caffeine inside the SBA-15 pores. PEO-PPO-PEO is poly(ethylene glycol)–poly(propylene glycol)-poly(ethylene glycol).[52]

3.5. Gastroesophageal reflux disease

3.5.1. Famotidine

Famotidine (FM) inhibits stomach acid production, and used in the treatment of peptic ulcer disease and gastroesophageal reflux disease.[53] Functionalization of SBA-15 with 2-cyanoethyltriethoxysilane followed by hydrolysis of the cyano groups to obtain SBA-15-Et-COOH. The maximum amount of FM loaded onto the SBA-15-COOH was 15 wt%.[54] Another publication investigated pH-responsive activity of FM/SBA-15 tablet coated with hydroxypropyl methylcellulose phthalate (HPMCP). In SGF (pH 1.2), the coating material could effectively delay the release rate of FM from SBA-15. But in SIF (pH 7.5), because the HPMCP is quickly dissolved into the neutral solution, it did not have an obvious effect on the drug delivery rate. Therefore, HPMCP/FM/SBA-15 (Scheme 10) is a good drug delivery system for treatment of gastric problems.[55]

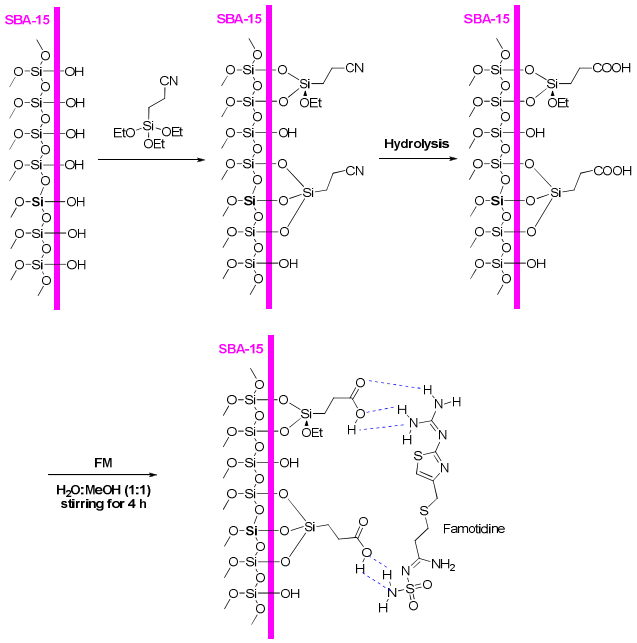

Scheme 9: The production and structure interaction of FM/SBA-15-COOH

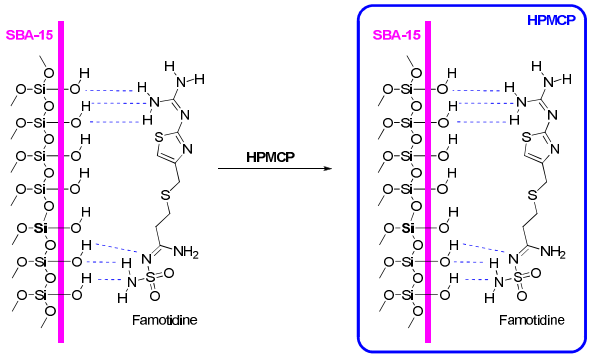

Scheme 10: The structure interaction of FM/SBA-15 and HPMCP coated FM/SBA-15

3.6. Cardiovascular and antihypertensive drugs

3.6.1. Atenolol

Atenolol (ATE) is a selective ß1 receptor antagonist, known as β-blocker drug, is used for treatment of hypertension and cardiovascular diseases.[56] Overdose of atenolol is very dangerous; hence, adjusting the dose of ATE becomes significant.[57] The *in vitro* drug release properties of ATE/SBA-15 matrix at 37 ºC for 10 hours is presented in Chart 2; it does not show a sharp initial release burst during the first hours. This system presents a low rate of delivery, followed by a rather constant rate over the subsequent hours with a linear regression factor of 0.999.[58]

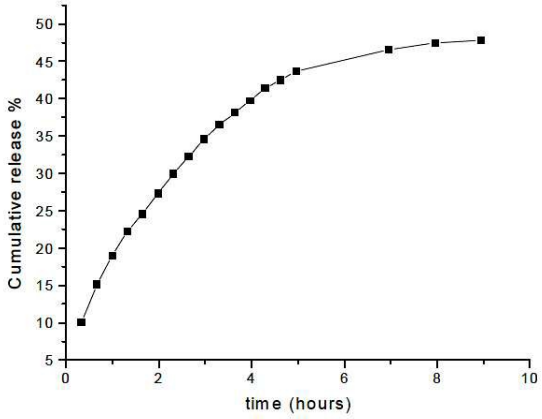

Chart 2: Cumulative release profile of ATE over 10 h[58]

SBA-15-collagen hybrid material was also synthesized by Cao[59] it was used as a delivery system for ATE.[60] The release kinetics of ATE/SBA-15 and ATE/SBA-15-

collagen presented a lower delivery rate during the first 10 h for both of them. After 10 h, the SBA-15 system appeared to be more effective than SBA-15-collagen. ATE/SBA-15 showed a release profile of almost 100% after 6 days of assays, in contrast, the total cumulative release from ATE/SBA-15-collagen at the end of immersion experiment was 80%. On the other hand, the presence of collagen in the SBA-15 matrix played an important role which affected on the ATE release from the mesoporous sample.

The other three types of SBA-15 carrier which were used in ATE include: Fe_3O_4/SBA-15,[61] PNIPAAm/SBA-15[62] and Fe_3O_4-PNIPAAm/SBA-15[63] hybrid systems. The formation of PNIPAAm into the mesoporous support provoked on a slight decrease in the pore volume and in the pore diameter (Table 3).

Table 3: The comparison of characteristics of various functionalized SBA-15

Name	BET surface area (m^2/g)	Pore diameter (nm)	Pore volume (cm^3/g)
SBA-15	789[61], 672[62]	6.2[61], 5.7[62]	1.329[61], 0.956[62]
Fe_3O_4/SBA-15	585[61], 413[63]	6.2[61], 6.5[63]	0.739 [61], 0.76[63]
PNIPAAm/SBA-15	326[62]	3.8[62]	0.484[62]
Fe_3O_4-PNIPAAm/SBA-15	171[63]	3.8[63]	0.35[63]

In Chart 3, the ATE release behavior of above carrier systems was separately showed. In part a, ATE release of Fe_3O_4/SBA-15 did not influence by an external magnetic field and after 10 h, release rate increased slightly (reached to 12%).[61] For PNIPAAm/SBA-15 (Chart 3, part b), ATE release was tested in different temperatures and showed that at 25-30 °C, release rate was high; it was decreased reasonably at 35 °C and with the increase in temperature, an increase in ATE release is observed. This behavior proves ATE-PNIPAAm/SBA-15 was a thermo-sensitive system that its LCST is around 35 °C.[62] In Chart 3 part c and d, the ATE release behavior of Fe_3O_4-PNIPAAm/SBA-15 and Fe_3O_4/SBA-15 was compared in the absence and presence of an external magnetic field, respectively. As mentioned before, by an external magnetic field the release of ATE from Fe_3O_4/SBA-15 did not affect, but from Fe_3O_4-PNIPAAm/SBA-15 affected by it; since the presence of a magnetic field provokes the heating of the nanocomposite material due to the vibration of the magnetic particles, the release of ATE molecules was enhanced. Also, based on the hyperthermia test, the maximum temperature obtained was around 40 °C inferior to that recommended for hyperthermia treatment. So, to

optimize the release of ATE-Fe_3O_4-PNIPAAm/SBA-15, the magnetic field amplitude, the frequency, or both of them should be reduced.[63]

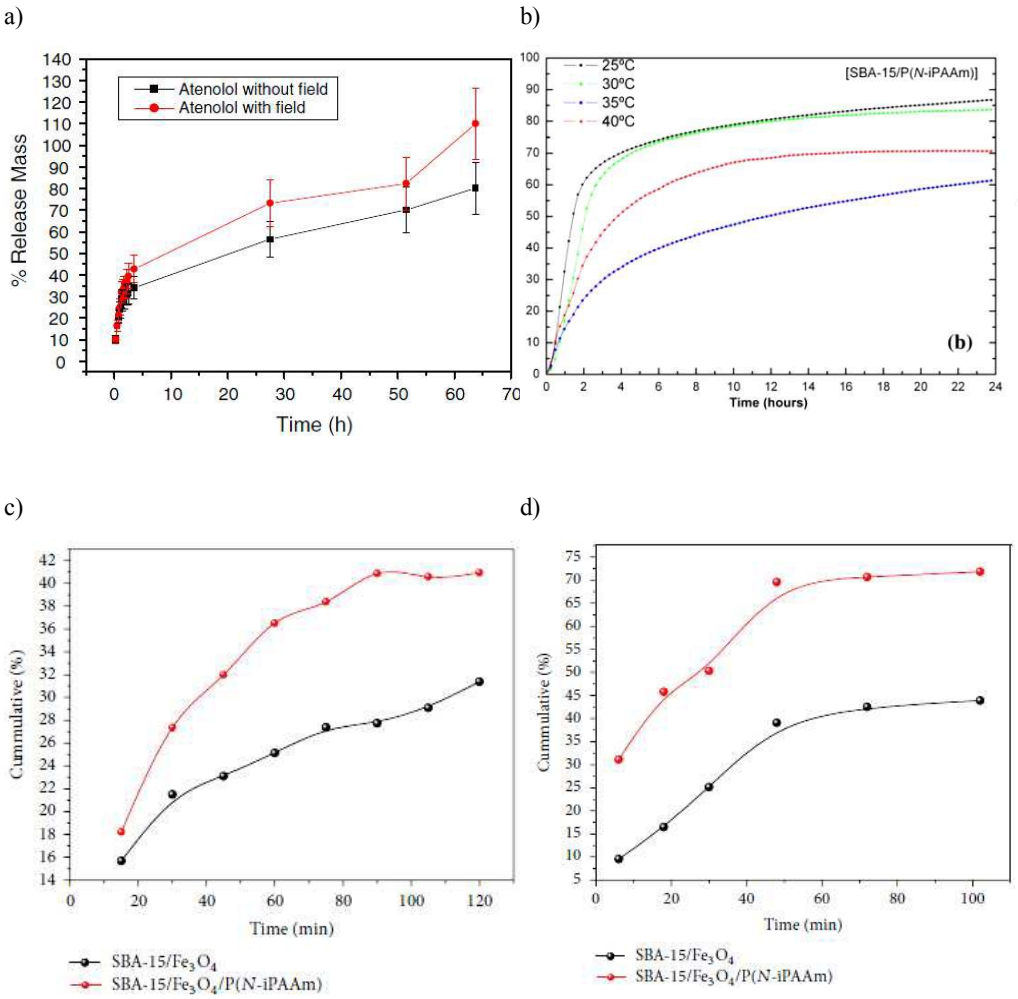

Chart 3: ATE release charts, a) ATE-Fe_3O_4/SBA-15 in the absence and presence of an external magnetic field.[61] b) PNIPAAm/SBA-15 in various temperatures.[62] c) Fe_3O_4-PNIPAAm/SBA-15 in the absence of magnetic field and d) in the presence of an external magnetic field.[63]

3.6.2. Captopril and Aliskiren

Captopril (CAP) with the size of 0.90×0.57×0.33 nm is an orally angiotensin-converting enzyme inhibitor used for the treatment of hypertension and some types of congestive heart failure. The three forms of calcined SBA-15, MgO/SBA-15 and SBA-Pr-NH_2 were applied for loading and release study of CAP. SEM images (Fig. 5) of CAP/SBA-15 and CAP-MgO/SBA-15 exhibited that the spherical particles of CAP are attached to

their external surface. SEM images also show that from those, MgO/SBA-15 apparently has stronger interaction with CAP molecules than pure SBA-15, which can be correlated with the basicity of magnesium oxide.[64] Release study of CAP/SBA-15 exhibited 60 wt% of the drug was suddenly released within 0.5 h, then, 78 wt% were released within 2 h, and almost completed the drug release over a period of 16 h.[65] The CAP-MgO/SBA-15 release profile showed that the drug release is relatively fast in the first 6 h (reached 89.3 wt% after 30 h), but significantly slower than that of CAP/SBA-15 due to the formation of stronger bonds between MgO and CAP molecule.[64] CAP/SBA-Pr-NH_2 release showed initially, as for the CAP/SBA-15, a burst release effect was visible for the first 6 h of the release period, followed by a second, very slow, release pattern. The burst release stage corresponds to the release of the CAP molecules placed on the external surface both of the SBA-Pr-NH_2 and MgO/SBA-15.[66] The same results were obtained by loading of aliskiren onto the MgO/SBA-15 pores.[64] Aliskiren is used for treatment of high blood pressure, but it is more harmful than beneficial.[67]

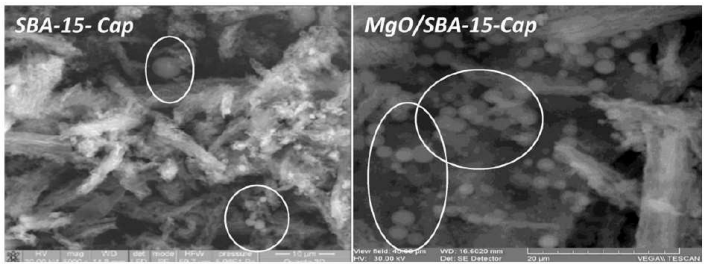

Fig. 5: SEM images of CAP/SBA-15 and CAP-MgO/SBA-15 exhibit that the spherical particles of CAP are attached to the external surface of them.[64]

3.6.3. Fenofibrate

Fenofibrate (FN) is a poorly water-soluble drug which is used to reduce cholesterol level in patients at risk of cardiovascular diseases. FN loading onto SBA-15 as carrier can help to drug's dissolution. Five methods were used for FN loading include: (i) physical mixing by blending FN and SBA-15, (ii) melting of FN over 80 °C in a mixture with SBA-15, (iii) solvent impregnation, and loading in a high pressure reactor by (iv) liquid CO_2 and (v) supercritical (SC) CO_2 methods. FN loading for the impregnation, liquid CO_2 and SC-CO_2 methods was indicative of the more homogeneous FN distribution. The mixing and melting methods resulted in enhanced

drug release compared to the impregnation, liquid CO_2 and SC-CO_2 methods producing the greatest increase at time of about 30 min. In addition, the similarity of the drug release profiles for the melt, impregnation, liquid and SC-CO_2 samples showed that the deposition behavior of FN in the SBA-15 did not adversely affect its release.[68]

3.6.4. Furosemide

Furosemide (FURO) is a loop diuretic used in the treatment of congestive heart failure and edema. It is a drug preferentially absorbed in the stomach with low water-solubility. Drug loading was measured by UV spectrophotometry and TGA and resulted 30.0 wt% for FURO/SBA-15. After 2 h the drug released was 71% from FURO/SBA-15 against the 49% released by the commercial product.[69]

3.6.5. Metoprolol

Metoprolol (MT), is used in the treatment of hypertension, was loaded onto the pores of modified SBA-15 (SBA-Pr-SO_3H). The maximum amount of loaded MT onto SBA-Pr-SO_3H was 4 wt% higher than pure SBA-15. The release profile of MT/SBA-15 reaches 95% after 10 h; however, it was 40% for MT/SBA-Pr-SO_3H at the same time. Finally, a complete release was found for MT/SBA-15, whereas in sulfonated sample certain amount was strongly anchored within the porous structure.[51]

3.6.6. Nimodipine

Nimodipine (NIM) is a dihydropyridine calcium channel blocker and widely used for the treatment of high blood pressure.[70] The NIM was doped inside the pores of the SBA-15 and then drug release process from the matrix into a SBF solution was studied. The NIM adsorption on the external surface of the SBA-15 was decreased by selective modification of the external surface of the SBA-15 using phenyl-trimethoxysilane or trimethylchlorosilane before calcination. It is expected that after calcination process, all of the outside silane can be oxidized off, but the silanol groups of the pore channels can be kept. The release effect of NIM was 50% in 12–13 h, 100% in 24–25 h and the process was made in an almost linear release pattern.[71]

3.7. Anti-fungal drugs

3.7.1. Itraconazole

Itraconazole (ITZ) is a triazole anti-fungal drug which is used for treatment of fungal infections. It is a routine drug model for investigation of release ability of new carriers.[7, 72] SBA-15 was loaded with ITZ using three different procedures: (a) adsorption from solution, (b) incipient wetness impregnation using a concentrated solution in CH_2Cl_2 followed by solvent evaporation, and (c) melting of ITZ in a mixture with SBA-15. The incipient wetness impregnation technique had the best result with the more uniform distribution onto the pores and a loading of 20% wt (Fig. 6). The *in vitro* release of ITZ was evaluated in an aqueous environment simulating gastric fluid and showed fast release kinetics.[73, 74] Furthermore, the stability of ITZ/SBA-15 upon humidity storage was investigated over one year period. Since the surface of the pores of SBA-15 undergoes hydroxylation at high relative humidity, hydrophilicity is enhanced and lead to improvement of ITZ release upon contact with water.[75] Release of ITZ from SBA the fasted states a supersaturated state in the fasted state simulated intestinal fluid (FaSSIF). The supersaturated state of ITZ subsequently provoked the formation of nanofibers with a width of 12 nm that prevents its transepithelial transport across a Caco-2 cell monolayer which mimics the gastrointestinal barrier. By the use of mixed micelles of FaSSIF, ITZ absorption is enhanced, but the formation of ITZ nanofibers prevented.[76]

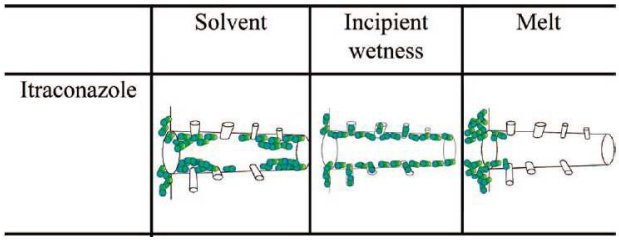

Fig. 6. Physical state of the ITZ distribution onto the pores of SBA-15 using different methods.[73]

3.7.2. Sertaconazole

Sertaconazole (SER) is an imidazole class of antifungal drug which is available as a cream to treat skin infections such as athlete's foot. Near about 63 wt% SER loaded onto the SBA-15 pores. A slow release pattern was observed for SER/SBA-15 and SER was

dissolved up to 98% in 5 h, while the pure SER was dissolved only up to 24% in 5 h. Furthermore, SER/SBA-15 has burst release (50%) within the first 30 minutes.[77]

3.8. Antibiotics

3.8.1. Cephalexin

Basaldella and Legnoverde synthesized functionalized SBA-15 with sulfonic acid and amine groups (SBA-15-Pr-SO_3H and SBA-15-Pr-NH_2, respectively) to study the effect of changes in the surface acidity on cephalexin (CPX) adsorption and subsequent release. *In vitro* release of CPX showed that the release rate (1-20 h) was strongly influenced by the nature of the anchored groups, the slower delivery rate obtained for CPX/SBA-15-Pr-NH_2. The release rate of CPX/SBA-15-Pr-NH_2 is lower than the other types of CPX/SBA-15 in all cases (Table 4) which proves a considerable interaction between CPX and SBA-15-Pr-NH_2 because of the presence of a carboxylic group in the drug molecule. In contrast, the fastest release was observed for CPX/SBA-15-Pr-SO_3H since there are not interactions occurred between the CPX molecules and the sulfonic acids on the surface, despite the presence of an amino group in the CPX molecule.[78] In another publication, it was demonstrated that, post-functionalization SBA-15-Pr-NH_2 could enhance the long-term CPX delivery in comparison with the co-condensation procedure.[79]

Table 4: Release percentage of CPX loaded onto the various SBA-15[78]

	CPX/SBA-15	CPX/SBA-Pr-SO_3H	CPX/SBA-Pr-NH_2
Release (%) after 20 h	75%	80%	~60%
Release (%) after 2 days	90%	90%	70%

Legnoverde *et al.* also published the study of pH influence on the CPX adsorption onto SBA-15. Their molecular modeling and docking calculations demonstrated that a cationic form of CPX (in acidic pH below 2.56) lead to the highest adsorption capacity since the formation of a NH_3^+ group of CPX interacts better with silanol groups of SBA-15.[80]

3.8.2. Gentamicin

Three different types of SBA-15 have been used for gentamicin (GEN) delivery include: pure SBA-15, PLGA/SBA-15 and γ-Fe_2O_3-PNIPAAm/SBA-15.[81-83] Based on the results in Table 5, pore diameter of γ-Fe_2O_3-PNIPAAm/SBA-15 and PLGA/SBA-15 is about 4.9 nm which is not big enough to accommodate the GEN (1.6 × 0.8 nm) effectively, so the GEN loaded onto their pores are lower than SBA-15. Nevertheless, the GEN release before 10 h was 80%, 40% and 70% for GEN/SBA-15, GEN-PLGA/SBA-15 and GEN-γ-Fe_2O_3-PNIPAAm/SBA-15, respectively. In addition, GEN-γ-Fe_2O_3-PNIPAAm/SBA-15 is a magenetic-thermo sensitive drug carrier which observed that an apparent increase of the release amount is happening between 30 and 40 °C; the maximal release amount only reached to 29% and 65% after releasing for 6 h at below 30 °C and at 40 °C, respectively.

Table 5: The comparison of characteristics of various functionalized SBA-15

Name	BET surface area (m^2/g)	Pore diameter (nm)	Pore volume (cm^3/g)
SBA-15 [81]	787	6.1	1.056
PLGA/SBA-15 [82]	-	4.9	0.789
γ-Fe_2O_3/SBA-15 [83]	374.8	6.5	0.492
γ-Fe_2O_3-PNIPAAm/SBA-15 [83]	124.8	4.9	0.155

3.8.3. Sulfadiazine

The surface of SBA-15-Pr-NH_2 was reacted with succinic anhydride to obtain carboxylic modified mesoporous carriers (SBA-15-COOH), then, sulfadiazine (SD) was chosen as a model drug (Scheme 11). The two step modification procedure resulted in a significant specific surface area and pore size decreases for both types of modified SBA-15. The amount of adsorbed sulfadiazine in SBA-15 and SBA-15-COOH was around 54% and 52%, respectively. After 4 h approximately the whole amount of SD was released from SD/SBA-15. In contrast, the slower release rate was observed from SD/SBA-15-COOH (25 h for totally release of SD); it is because of the formation of COO^--NH_3^+ between SBA-15-COOH and SD molecules that is stronger than the interaction between silanol groups of SBA-15 and SD molecules. In addition, SD/SBA-15-COOH did not increase cytotoxicity on Caco-2 cell line suggesting that the obtained modified carriers were biocompatible.[84]

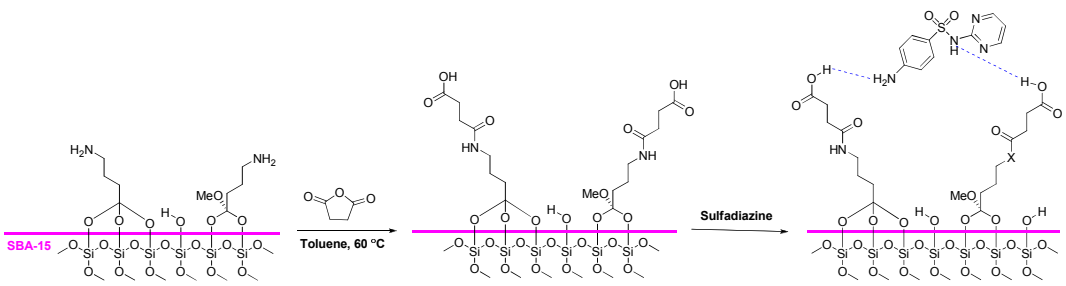

Scheme 11: SBA-15 surface modification with carboxylic acid group and its interaction with SD molecule

Silver sulfadiazine (AgSD) is a topical antibacterial cream for treatment of burn wound infections, but, unfortunately, it has poor solubility in water.[85] Szegedi and coworkers found that SBA-15 can be easily modified by direct or post-synthesis methods to prepare Ag nanoparticles inside the channels or on its outer surface (Ag/SBA-15). In addition, the silica host can stabilize Ag nanoparticles and water-soluble silver ions are released. Then, the empty pores of pure SBA-15 and Ag/SBA-15 adsorbed the AgSD and SD molecules, respectively, and the results were compared. AgSD/SBA-15 significantly improved its water solubility; furthermore, comparing the SD release and antimicrobial properties, AgSD/SBA-15 can be effectively replaced by SD/SBA-15 or SD-Ag/SBA-15 materials.[86]

3.8.4. Vancomycin

Vancomycin (VAN) is a large natural glycopeptide antibiotic (1.8×1.5×1.0 nm) which is used for treatment of number infections.[87] The adsorption and release of VAN from SBA-15 materials have been tested as a function of the surface properties, chemical structure and pH variations. For this aim, the SBA-15 surface has been modified with various functions include: *N*-(2-aminoethyl)-aminopropyldimethoxymethylsilane (APMS), 3-mercaptopropyltrimethoxysilane (MPTS),[88] octyltrimethoxysilane (OTMS)[89] and 11-triethoxysilanylundecanoic acid ethyl ether (TSDAE).[90] In comparison of VAN loaded onto the SBA-15, SBA-15-APMS and SBA-15-Pr-SH, since adsorption depends on the direct chemical interaction between the mesopore surface and VAN molecules.[88] Investigation of SBA-15-C_8H_{17} exhibited that it released the VAN at a much lower rate than pure SBA-15 that released quantitatively the antibiotic in only 3 h.[89] Yang *et al.* examined VAN storage and release of SBA-15 and

SBA-15-($C_{10}H_{20}$)COOH in the absence and presence of poly(dimethyldiallylammonium chloride) (PDDA). The results in Table 6 show that the maximum amount of VAN was stored onto the SBA-15-($C_{10}H_{20}$)COOH up to 36.4% in the presence of PDDA at pH 6.8. Moreover, the released amounts of VAN from VAN/SBA-15-($C_{10}H_{20}$)COOH were gradually increased from 8 to 86% by adjusting the pH values from 6.5 to 2.0.[90] In spite of all these data, Cauda and coworkers demonstrated that pure SBA-15 fibers cannot adsorb VAN molecule, but SBA-15 spheres can. They mentioned that it induced by the low accessibility of mesopores which are partially closed at the fiber ends.[91] A composite of delivery system for vancomycin, rifampicin and linezolid has been designed for the treatment of bone infection in which the most active antibiotic after loading and release was vancomycin.[92]

Table 6: The comparison of characteristics of various functionalized SBA-15

Name	BET surface area (m^2/g)	Pore diameter (nm)	Pore volume (cm^3/g)	Drug loaded (%wt)
SBA-15 [88]	956[a]	10.5[a]	1.26[a]	5.0
SBA-15-APMS [88]	350[a]	8.91[a]	0.587[a]	24.0
SBA-15-Pr-SH [88]	639[a]	9.31[a]	0.874[a]	5.0
SBA-15-C_8H_{17} [89]	594[a,b]	4.7[a,b]	0.023[a,b]	13.4[c]
SBA-15-($C_{10}H_{20}$)COOH [90]	544	7.2	1.02	-
VAN-PDDA/SBA-15-($C_{10}H_{20}$)COOH [90]	190	5.9	0.40	36.4
VAN/SBA-15-($C_{10}H_{20}$)COOH [90]	528	7.2	0.97	5.0
VAN-PDDA/SBA-15 [90]	534	7.2	1.00	2.2

[a]Before loading of VAN
[b]The S_{BET}, pore diameter and volume of its mother SBA-15 was 700 m^2/g, 5.7 nm and 0.027 cm^3/g, respectively.
[c]10.5% for pure SBA-15

3.8.5. Amoxicillin

Amoxicillin (AMX), a β-lactam antibiotic, incorporated into the porous calcined SBA-15 by contacting its solution in an appropriate solvent with the porous solid, and the drug release process from the matrix into a SBF solution has been studied. It was found that AMX/SBA-15 composite is strongly dependent upon the solvent acidity. With the raising of the solution pH to 7, the AMX adsorption was greatly enhanced and reached to a value of 24 wt% under optimum conditions. Also, AMX release from the composite in the form of powder was faster than the disk form.[93]

Sevimli and Yılmaz studied pure SBA-15, SBA-15-Pr-SH, SBA-15-Pr-NH_2 and caped SBA-15 (with triethoxy methyl silane) as carriers for AMX delivery. As it is illustrated in Table 7, SBA-15-Pr-SH adsorbed AMX with the maximum value (27.5%) while the SBA-15-Pr-NH_2 could adsorb less AMX such as 18.3%. AMX is a water-soluble drug which makes it easier to load it within SBA-15-Pr-SH particles with less hydrophilic properties. The HPLC method was also used to plot the release profile which indicated that the release is sustained rather than prolonged and the functionalization does not affect the controlled release of AMX (Table 7).[94]

Table 7: The comparison of various SBA-15 for loading and releasing of AMX[94]

Sample	Loaded AMX (wt%)	mg released AMX (a. u.) after 30 min
AMX/SBA-15	22.3	~ 40
AMX/SBA-15-Pr-NH_2	18.3-20.7	70
AMX/SBA-15-Pr-SH	22.9-27.5	170
AMX/SBA-15-caped	20.8-27.2	120

3.8.6. Tetracycline

Tetracycline (TC) may be adsorbed onto the surface of SBA-15-Pr-NH_2 by hydrogen bonding between NH_2 groups of modified SBA-15, C=O and OH groups of the TC molecules. The maximum amount of TC loaded onto the SBA-15 and SBA-15-Pr-NH_2 was 20.6 and 42.3 wt%, respectively. *In vitro* release TC revealed that TC/SBA-15-Pr-NH_2 has a slower release rate than TC/SBA-15, especially at pH=7.4 and 4.8. However, the burst release occurs at pH=1. 2 as a result of protonation of amino groups on the modified SBA-15 and so, the formation of the repulsive forces between SBA-15-NH_2 and TC molecules.[95] Vu *et al*. showed that pure SBA-15 does not adsorb TC molecules as there are no interaction between TC and surface sites [96]. Hence, Das and coworkers designed SBA-15 like mesoporous phosphosilicate that was able to form a core–shell–corona architecture and encapsulation of TC molecules due to the presence of phosphonium cations.[97]

3.8.7. Macrolides antibiotics

Macrolides are another family of antibiotics that are widely utilized for infections. Erythromycin (ERY) and clarithromycin (CLA) are both classified as macrolide antibiotics. ERY is a pure antibiotic derived from a certain microorganism while CLA is a semi-synthetic macrolide antibiotic (6-O-methylerythromycin).[98] Calcined SBA-15 and functionalized SBA-15 with octyltrimethoxysilane (SBA-15-C8) and octadecyltrimethoxysilane (SBA-15-C18) were used to evaluate ERY loading and delivery. Two different solvents were used in the preparation of SBA-15-C18 includes toluene (T) and acetonitrile (Ace). It is interesting to observe that SBA-15-C18(Ace) with the lowest surface area contains as much ERY as the other ones. This behavior offers that the C18 chain functionalized SBA-15 strengthens the interaction between the ERY and surface of matrix mesoporous. Thus, an effective controlled release of ERY has been achieved by functionalized SBA-15 with hydrophobic long chain hydrocarbon moieties. Based on the ERY release studies, the release rate decreases strongly for SBA-15-C18(Ace) which demonstrates the effect of used solvent in the functionalization process.[99]

Table 8: the comparison of the characteristics of various functionalized SBA-15[99]

Name	BET surface area (m^2/g) {after loading}	Pore diameter (nm) {after loading}	Pore volume (cm^3/g) {after loading}	Drug loaded (%wt)
SBA-15	787 {250}	8.8 {7.2}	1.06 {0.39}	34
SBA-15-C8	559 {271}	8.2 {6.1}	0.83 {0.50}	13
SBA-15-C18(T)	535 {182}	8.3 {5.5}	0.83 {0.34}	18
SBA-15-C18(Ace)	71 {8}	5.4 {-}	0.19 {0.04}	15

Additionally, tris(2-aminoethyl)amine functionalized SBA-15 (SBA-15-TREN) was selected as the carrier for CLA which could adsorbed it with 46 wt% at pH=8. The release rate of CLA was fast at pH 1.3, and the release amount basically reached a maximum value of 97 wt% after 210 min. In contrast, at higher pH, the release was quite low and remains essentially constant (13.0 wt% at pH 7.4).[100]

3.8.8. Allyl isothiocyanate

Allyl isothiocyanate (AITC) is a liquid organosulfur compound which extracted from mustard seeds and used as an insecticide and bactericide.[101] Two types of SBA-15, synthesized from two different mole ratios of its constituents, were used for the study of

their ability in the adsorption and controlled release of AITC. Whole pores were almost filled with the vapor phase of AITC (100%). However, burst released was observed for both SBA-15, more than 50% of the adsorbed phase was released in the first 12 h. The antimicrobial activity of the released (vapor-phase) AITC in comparison with liquid AITC in tests with some microorganisms verified that the lethal activity of the released AITC against these microorganisms was unaffected by adsorption and desorption processes.[102, 103]

3.9. Bisphosphonate drugs

Bisphosphonate drugs are widely used for treatment of those diseases with osteoarticular disorders such as osteoporosis, Paget's disease and osteolytic tumors.[104] It has been proved that less than 1% of the total orally administered drug amount reaches the bones because of the rapid release of bisphosphonates from the blood. Two types of bisphosphonate drugs, which were incorporated onto the SBA-15, include zoledronic acid (ZOL) and sodium alendronate (ALE) (Scheme 12).[105]

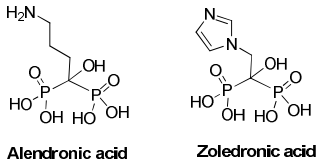

Scheme 12: The structure of sodium alendronate and zoledronic acid

3.9.1. Sodium zoledronate

Vallet-Regi and coworkers used pure SBA-15 and a composite of carbon nanotubes (CNT) over SBA-15 as carriers for ZOL. CNT/SBA-15 was simply synthesized by adding CNT material to the mixture of SBA-15 precursors during the preparation.[106] As shown in Table 9, the presence of the CNT and ZOL in the pores of SBA-15 caused to the decreasing of the BET surface. ZOL/SBA-15 release profile denoted that there was a burst desorption at the beginning of the experiment, followed by a more stationary release. After 192 h, it reached to completely release.[106, 107] The presence of the CNT in the structure of SBA-15 converts it to a conductive composite which allows applying an external electrical stimulus to influence cell biological responses. Although, ZOL release from CNT/SBA-15 followed the typical pattern of SBA-15-like materials,

metabolism of bone cell was stimulated and mitochondrial activity was increased up to seven times in the presence of ZOL-CNT/SBA-15 under electrical stimulus.[106]

Table 9: The characteristics comparison of SBA-15 and CNT/SBA-15

Name	BET surface area (m^2/g) {after loading}	Pore diameter (nm) {after loading}	Pore volume (cm^3/g) {after loading}
SBA-15 [107]	903 {250}	7.4 {7.4}	1.21 {0.56}
CNT/SBA-15 [106]	848-226[1]	not reported	1.26-0.99

[1]variation is based on the amount of CNT concentration

3.9.2. Sodium alendronate

Pure SBA-15, SBA-15-Pr-NH_2 and phosphorus-containing SBA-15 mesoporous materials have been tested as alendronate delivery systems. Phosphorus-containing mesoporous materials with SBA-15 type (PO_4/SBA-15) structure were obtained using the addition of H_3PO_4 during synthesis of SBA-15.[108] Drug delivery from ALE/SBA-15, ALE-PO_4/SBA-15 and ALE/SBA-Pr-NH_2 is fast in the initial testing time and achieves a stationary state after around 10 h of analysis. In addition, the maximum percentage of delivering ALE reached to 60% in about 20 h from pure or amino functionalized SBA-15. This is attributed to the partial retention of drug molecules onto the mesopores. In addition, ALE released after 24 h increased with the phosphorus incorporation, which could allow modulating ALE dosage according to the patient's clinical needs. This behavior is explainable by the increase of the chemical interactions between ALE molecules and SBA-15 matrix due to the incorporation of PO_4 units into the silica framework (Scheme 13). Also, the obtained results by the soaking of ALE-PO_4/SBA-15 in SBF after 14 days showed that the complete release of the drug would be possible before the formation of apatite-like layer onto the material's surface, which could difficult the drug diffusion and its pharmacological action.[109, 110]

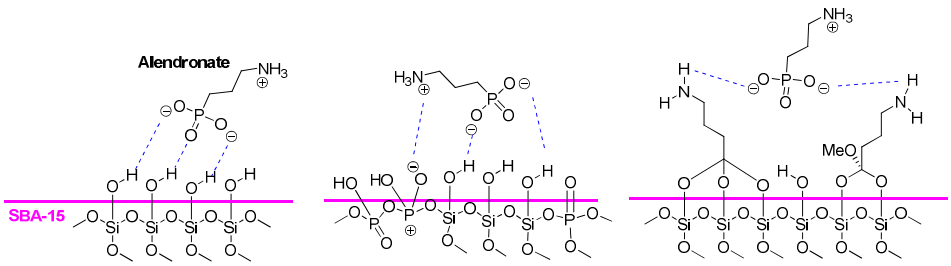

Scheme 13: The interaction between ALE and surface of SBA-15 (left), PO_4/SBA-15 (middle) and SBA-Pr-NH_2 (right)[109]

3.10. Proteins, enzymes and hormones

3.10.1. Bovine serum Albumin (BSA)

The oral immunization of vaccines allows easy administration, with a low risk of contamination, and reduced cost and with enhanced patient compliance. But, acidic gastric pH and proteolytic enzymes create a harmful environment that destroys the activity of vaccines and resulted in a poor immune response. Hence, the development of novel oral vaccine carrier systems would be very useful.[111] Serum albumin is the main protein of human blood plasma, which regulates the colloidal osmotic pressure of blood. Also, albumin transports fatty acids, hormones and buffers pH. BSA is a serum albumin derived from cows with a hydrodynamic diameter of around 7.2 nm and often used as a model antigen and protein concentration standard in lab experiments.[112]

SBA-15 was used as carrier for BSA to estimate its ability to develop of vaccine delivery. The amount of BSA adsorbed by SBA-15 was about 20 μg/mg which may be limited due to the steric hindrance of the BSA. In addition, 47% of BSA were released from BSA/SBA-15 at pH 7.4 after 24 h, and 90% of BSA were released at the end of the 4 days.[113] Nguyen *et al.* synthesized large pore size of SBA-15 using 1,3,5-trimethylbenzen as swelling agent, it was then functionalized with amino groups to separate of adsorbed-BSA effectively. The maximum adsorption capacity was increased since BSA (neutral) has a strong affinity for SBA-15 (negatively charged) *via* electrostatic bonds. The adsorption capacity increased with temperature indicates that the adsorption of BSA on SBA-15 is an endothermic process. The amount of BSA released by large pore size BSA/SBA-15-Pr-NH_2 reached to 65% in neutral pH, whereas the amount was around 80% at pH 10.[114] According to the results of Song *et al*., the release rate of BSA from BSA/SBA-15-Pr-NH_2 was very high and all the adsorbed BSA was released completely within 3 h.[22] In another publication, BSA/SBA-15-Pr-NH_2 was encapsulated with a thin layer coating of poly(acrylic acid) (PAA). BSA was released from the PAA/BSA-SBA-15-Pr-NH_2 at the higher pH value of 7.4 rather than at the lower pH value of 1.2. This system as a pH-sensitive carrier has a potential

application in the release of BSA to the site of higher pH value, such as small intestine or colon.[115] in addition, the composition of SBA-15 with anodic alumina membranes (AAMs) was used as deliver for BSA. The composite was simplicity synthesized by the addition of AAMs to a mixture of SBA-15 precursors. The constant release profile of BSA was obtained in BSA/SBA-15-AAM which release rate was about 2 μg/day. The total released quantity was around 70% of the BSA loaded in the SBA-15-AAM composite.[116]

3.10.2. Urate oxidase (an enzyme)

The urate oxidase (UO) catalyzes the oxidation of uric acid to 5-hydroxyisourate and allantoin. It can be used to treat diseases like hyperuricemia, gout and uric acid nephropathy by oxidation of uric acid to allantoin as a more water soluble and easily extractable compound.[117] SBA-15 was chosen as carrier for delivery of UO. The maximum amount of adsorbed UO onto the SBA-15 was obtained in the absence of permeation enhancer up to 33 wt%. UO/SBA-15 showed the constant release rate and the release was completed after 35 h. Furthermore, the UO/SBA-15 permeated in small quantities through rat skin while through human skin was permeable in the presence of oleic acid. Thus, this combination of nano SBA-15 and enzyme can offer a better treatment of uric acid disorders.[118]

3.10.3. Lyzozyme

Lyzozyme (LYS), a glycoside hydrolases enzyme, is a part of the innate immune system and acts as a natural antibiotic. LYS Deficiency in the infant's diet can lead to the incidence of diarrhea and bronchopulmonary dysplasia.[119] Although pure SBA-15 was used for LYS adsorption and delivery, it was not effective compared MSE (a type of organosilane) for this aim. Also, about 60 wt% adsorbed LYS on SBA-15 did not release and remained on the surface of silica.[120] LYS release from LYS/SBA-15 is enhanced by the swelling of the channels due to the nucleophilic attack of water to siloxane groups, thus, functionalization of the SBA-15 surface is a good procedure to enhance the structural stability. Various types of amino functionalized SBA-15 were used to investigation of their LYS delivery ability, include aminopropyltriethoxysilane (SBA-NH_2), *N*-2(-aminoethyl)-3-aminopropyltrimethoxysilane (SBA-15-diamine), and

(3-trimethoxysilylpropyl)diethylenetriamine (SBA-15-triamine). Since the adsorption of the LYS molecules on the amino-SBA-15 surface is governed by both hydrophobic and electrostatic interaction, the release amounts are different for each sample. The release amount of LYS from SBA-15-diamine was higher than the other samples. It exhibited an initial burst release before 5.5 h (62 wt%), however, completely released obtained after 90 h which make it a desire carrier for LYS delivery. For the SBA-15-NH_2 and SBA-15-triamine the maximum LYS release reached to 60 and 40 wt%, respectively. Thus, A substantial amount of the LYS remained on the surface of silica.[121]

3.10.4. Hydrocortisone

Hydrocortisone (HC) is the pharmaceutical name for cortisol, which is one of the most important steroids produced by the human body. It is one of the most common drugs used as an immunosuppressive drug. The four types of SBAs were synthesized and then loaded with HC. One is a simple SBA-15; two others were modified SBA-15 using 1,3,5-trimethylbenzene as additive, and the fourth one was prepared using NaI as additive. Just the 4th sample was basically disordered; the other ones were ordered hexagonal nanotubes with different pore size. Release rate investigation showed at 26 hours, the forth SBA-15 samples delivered 93%, 88%, 84%, and 61% of the HC, respectively. Thus, the first three SBA-15s have released most of the HC during this time and only a small amount of the HC remained with them. In contrast, the 4th SBA-15 still has around 40% of the drug after the initial (26 h) fast delivery period. It shows that the release kinetics can be strongly influenced by the using of different co-additives during SBA-15 synthesis.[122]

3.10.5. Progesterone

β-Cyclodextrin (β-CD) modified SBA-15 is a pH-sensitive carrier for delivery of progesterone (PG). PG is another type of steroidal human hormone which is used widely for prevention of preterm birth. In the first approach, SBA-15 surface was functionalized with 3-glycidyloxypropyltrimethoxysilane to obtain an epoxide ring functional group on mesoporous silica. Then, mono-6-deoxy-6-mercapto-β-cyclodextrin reacted with epoxide on the SBA-15 to prepared SBA-15-β-CD-1. In the second approach, SBA-Pr-SH reacted with monotosylated β-CD to give SBA-15-β-CD-2. *In*

vitro PS release investigation were carried out at pH 1 (simulated gastric fluid) for 2 h and then at pH 6.8 (simulated intestinal fluid) using the pH change method. In acidic solution the release rated was increased since the solubility of PG adsorbed on the external surface increased. In addition, For PG/SBA-15-β-CD-2 system, PG loaded both on the external surface of the mesoporous SBA-15 and in the CD basket. This composite allows only diffusion of PG adsorbed on the external surface at acidic pH and the release is then completed after 2 h when the pH reach neutral values with both hybrid materials.[123]

3.10.6. Methylprednisolone hemisuccinate

Methylprednisolone (MP) is one of the most used and effective corticoids with anti-inflammatory properties. A particular application of MP is based on the treatment of rhinosinusitis. Different two-dimensional (2-D) and three-dimensional (3-D) mesostructured materials were employed to investigation of delivery ability of MP include MCM-41, SBA-15, expanded SBA-15, FDU-12, and SBA-16. SBA-16 exhibited high drug adsorption capacities and a slower delivery trend of MP was observed for all the materials, which is more pronounced in the case of SBA-15 and SBA-16.[124]

3.10.7. Insulin

Insulin (INS) is a peptide hormone produced by the pancreas. When control of INS levels fails, diabetes mellitus can result. Therefore, insulin is used for treatment of some forms of diabetes mellitus. The INS in monomer form has a molecular radius of 1.34 nm,[125] so it has suitable size to load in SBA-15 pores. Drug loading capacity and releasing of INS in simulated gastric and intestinal fluids were investigated by Siavashani and coworkers. UV-Vis results showed that about 14.8 percentage of insulin was loaded at SBA-15. Also, about 18.5% of insulin release at gastric tract and more than 14% release at intestinal tract during 120 and 400 h, respectively.[126]

3.11. Antidiabetic drug

Jin and coworkers synthesized pH-sensitive dual drug delivery system by coating of SBA-15 with Poly(sodium4-styrenesulfonate) (PSS) and Poly(diallyldimethyl-ammonium chloride) (PD). Then, PSS/PD/SBA-15 was used as carrier for both of metformin hydrochloride (MH) as an oral of antidiabetic drug and IBU. The loaded amount of MH onto the mesopore was 10 wt% and for IBU was 20 wt%. The MH release rate was very fast at pH 1.2 with an initial burst release at 0.5 h to reach 45% while IBU release very few. But in alkaline condition (pH = 8), the release of MH decreases only 18% within 72 h. On the contrast, IBU can be released freely in alkaline medium. Thus, MH and IBU release can be achieved by the pH changing of the surrounding environment.[127]

3.12. Anticancer drugs

3.12.1. Doxorubicin

Doxorubicin hydrochloride (DOX), a potent antibiotic, is commonly used to treat some types of cancers. Cardiomyopathy is the most dangerous side effect of doxorubicin, leading to congestive heart failure, due to the lack of ability to target cancer cells.[128] Folic acid (FA) has high binding affinity to the FA receptors on the surface of tumor cells. Silica surface can be modified with folic acid by a carboxylic acid functional group of FA. Pang *et al.* prepared poly(ethyleneimine)/SBA-15 (PEI/SBA-15) by the polymerization of aziridine on the surface of SBA-15.[129] Then, FA molecules reacted with amino groups of PEI-SBA-15 to obtain a targeted carrier FA-PEI/SBA-15 (Fig. 7). Finally, DOX was loaded in the SBA-15, PEI/SBA-15, and FA-PEI/SBA-15 up to 8.7 wt%, 4.0 wt%, and 3.5 wt%, respectively. The decreased drug loading content after modification can be explained by decreasing pore size and increasing of the repulsion between silica surface and DOX molecules. *In vitro* cytotoxicity shows that the empty FA-PEI/SBA-15 particles have a lower cytotoxicity in comparing with the PEI/SBA-15 particles. In addition, the DOX-FA-PEI/SBA-15 particles exhibited excellent anticancer effect to HeLa cells than the pure DOX and DOX/SBA-15 particles due to the presence of FA receptors.[130]

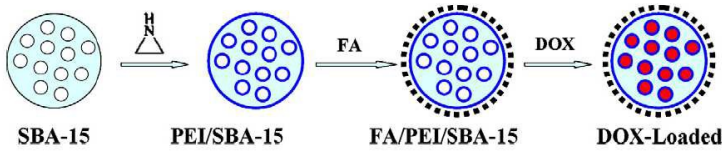

Fig. 7: Procedure for preparation of DOX-FA-PEI/SBA-15[130]

3.12.2. Gemcitabine

Pure SBA-15 and amino functionalized SBA-15s with APTES (SBA-15-NH_2), 3-[bis(2-hydroxyethyl)amino]propyl triethoxysilane (SBA-15-$N(OH)_2$) and 3-[2-(2-aminoethylamino) ethylamino]propyl trimethoxysilane (SBA-15-N3) were tested as carriers for delivery of Gemcitabine (GM). Based on the results in Table 10, the surface functionalization led to the loading enhancement of GM in which SBA-15-NH_2 has the maximum amount of loading content. The release rate of the amino modified samples was pH dependent; it reached up to 60%, 43% and 65% after 24 h at pH 5.6 in comparison to 27%, 14% and 33% at pH 7.4 for GM/SBA-15, GM/SBA-15-NH_2 and GM/SBA-15-N3, respectively. The release profile of GM/SBA-15-N $(OH)_2$ was completely pH independent because of difficult protonation of OH groups in acidic solution.[131]

Table 10: loading content of GM on silica surfaces[131]

Sample	Loading content of GM (%)
GM/SBA-15	7
GM/SBA-15-NH_2	21.65
GM/SBA-15-$NH(OH)_2$	19.58
GM/SBA-15-N3	6

3.12.3. Dasatinib

Two types of SBA-15 were synthesized by Kjellman *et al.* include one standard SBA-15(micro-meso) and one with reduced intra wall porosity SBA-15(meso). Then, the drug dasatinib (DT), as a tyrosine kinase inhibitor, was loaded into the pores of both materials. The loaded DT was 17 and 15 wt% for DT/SBA-15(micro-meso) and SBA-15(meso), respectively. Release profile of the DT/SBA-15(micro-meso) and DT-SBA-15(meso) exhibited that between 70–95% of the loaded DT were initially released. It is worth noting that a more rapid release rate was observed for the loaded DT during the

initial burst as compared to that of the free DT. It is because of DT easy access to the solvent and that the kinetics of dissolution are even faster than for the free DT. The lack of micropores not only led to a higher initial release, but also followed by a rapid drop in the concentration of releasing drug.[132]

3.12.4. Methylphenyltin dichloride

Pyridine modified surface of SBA-15 (SBA-15-Py) can be prepared using reaction with *N*-[3-(triethoxysilyl)propyl]isonicotinamide. The pyridine at the surface of the SBA-15 pore played a role as a ligand to coordinate with Methylphenyltin dichloride (MPSn) and resulted in the formation of a stable adduct complex (Scheme 14). The adsorption was completely pH dependent; in acidic solution, pyridine groups react with H^+ and convert to pyridinium ions and result in a decrease of its coordination ability. In addition, the SBA-15 structure is sensitive to high pH value and become damaged, thus, pH was the optimized condition for loading the drug. It was found that MPSn was completely released from SBA-15-Py at acidic pH (pH 1.6 HCl) similar to stomach fluid, but releasing in SBF was at a minimum which is corresponding to the mouth. It can be concluded that this is a suitable delivery system for oral metal-base drug delivery such as tin complex.[133]

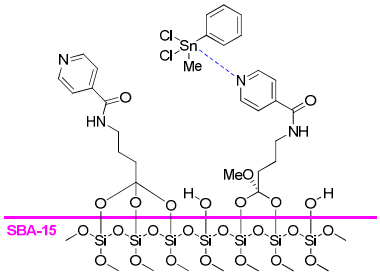

Scheme 14: complex structure of PMSn/SBA-15-Py

3.12.5. Cisplatin

Vathyam *et al.* showed that drug incubation temperature, methods of surfactant templates removing from the mesoporous materials and solvents used for modification of surface can affect the adsorption capacity and the drug release rate. They investigated the adsorption and release properties of Rhodamine 6G (R6G) and cisplatin as a tracer dye and anticancer drugs, respectively, using different conditions and various types of

mesoporous materials. PMO (periodic mesoporous organosilica), MCM-41 and SBA-15 were used and interestingly, the PMO showed a significantly higher adsorption capacity for both R6G and cisplatin than the MCM-41 or SBA-15.[134]

3.12.6. Methotrexate

The feasibility of SBA-15, MCM-41, LDH (layered double hydroxide) (Mg_3Al-NO_3) and MC (mesoporous carbon) were comparatively evaluated for oral drug delivery of methotrexate (MTX). MTX is used widely to treat neoplastic diseases such as acute lymphoblast leukemia, lymphoma and solid cancers and autoimmune diseases. The toxicity evaluation based on Kärber method exhibited that the synthesized host matrices and nanocomposites are practically non-toxic. UV-Vis absorption spectra of MTX solutions after loadings on mesoporous materials showed that SBA-15 and MCM-41retained the largest and the smallest amount of MTX, respectively (MCM-41 < LDH < CM < SBA-15). As shown in Table 11, MTX/SBA-15 has the lower released MTX quantities after 4 h and also 1 day. In all cases, the released amount of MTX from the mesoporous matrices is lower than commercially available drug.[135]

Table 11: release profile of MTX[135]

Sample	Release amount after 4 h (wt%)	Release amount after 1 day (wt%)
MTX/SBA-15	18.6	55
MTX/LDH	22.6	75
MTX/MC	21.8	85
MTX/MCM-41	30.5	88
Commercial MTX	54.2	95

3.13. Anticonvulsant drugs

3.13.1. Kynurenic acid

Kynurenic acid (KYN) is a product of the normal metabolism of amino acid L-tryptophan. It has neuroactive activity and acts as an antiexcitotoxic and anticonvulsant.[136] KYN was loaded onto the SBA-15 pores and its release profile exhibited a first stage of fast drug release followed by a slow release phase. In the first stage, 20% of KYN were released from the SBA-15 material within a period of 24 h.

After this time, the release became slower because more time is needed to diffuse KYN molecules through the channels of SBA-15 structure.[137]

3.13.2. Carbamazepine

Carbamazepine (CBZ), a poorly water-soluble drug for treatment of seizure disorders, was loaded into SBA-15 *via* a wetness impregnation method and then processed by extrusion/spheronization into pellets to improve flow-ability CBZ/SBA-15. The maximum amount of CBZ loading in SBA-15 pores was determined to be 20% wt. Then, CBZ-release profiles for the CBZ/SBA-15 powder and pellet forms were compared with those from the corresponding physical mixture and pure crystalline CBZ After 30 minutes, release from the CBZ/SBA-15 powder and pellets reached 88.58% and 85.83%, respectively, versus only 34.23% and 57.00% from crystalline CBZ and the physical mixture, respectively. Thus, there is no difference between release from pellets and powder forms and incorporation into pellets did not change the release behavior of CBZ from the SBA-15 carrier. Furthermore, CBZ/SBA-15 pellets showed improved dissolution compared with crystalline CBZ *in vitro*, and significantly increased the oral bioavailability of CBZ *in vivo* as compared with CBZ tablets.[138]

3.13.3. Valproic acid and sodic phenytoin

López and coworkers investigated the loading and the neurohistopathology effect of valproic acid (VPA) and sodic phenytoin (SP) onto the SBA-15, separately. VPA is used in the treatment of epilepsy, bipolar mania and migraine prophylaxis.[139] Phenytoin is also believed to treat seizures by causing voltage-dependent block of voltage-gated sodium channels.[140] Based on the results obtained by N_2 adsorption–desorption isotherms, the final weight content of drug in the SBA is smaller for SP/SBA-15 than for VPA/SBA-15 (9% vs. 31.7%). Then, the local effect of the carrier implants was studied in the close vicinity with the rat brain near tissue by means of stereo tactic surgery. Six months later, the histopathology study of the tissue showed a histological section pointing out the position of the SBA-15 capsule at the hippocampus. As one can see from Fig. 8, the implant did not cause necrosis and inflammation and it show a good biocompatibility of the VPA/SBA-15 or SP/SBA-15 with brain tissue.[141]

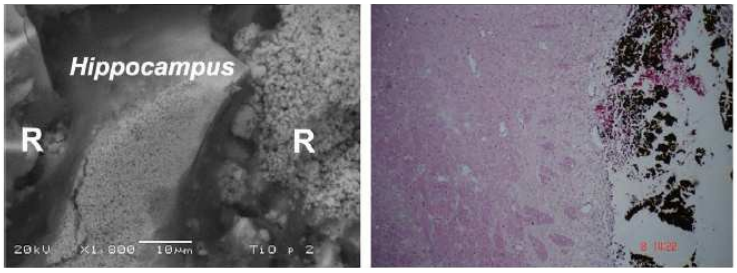

Fig. 8: Histopathology study of the tissue in contact with carriers. Left: Histological section of the hippocampus in the vicinity of the reservoir (marked as R). Right: Stained section micrograph of the neurons close to the silica capsule (shown in black).[141]

4. Conclusion

In summary, we gave an overview on the application of pure and modified SBA-15 as an efficient carrier for adsorption and delivery of various natural and chemical pharmacies. Hexagonal structure, large pore size, high surface area, great pore wall thickness, and high thermal stability are significant properties of these materials. Functionalized SBA-15 is more stable than pure SBA-15 in organic media. Formation of hydrogen bonds between silanol groups of SBA-15 and drug is the most common cause of drug adsorption, whereas physical interaction of functional groups between the drug and the functional groups on the surface of modified SBA-15 makes stronger adsorption on the modified surfaces. Magnetic SBA-15 makes it easier to separate in the presence of external magnetic fields and so is a good candidate for drug delivery. Also, the composition of drug/SBA-15 coated with a pH-responsive polymers causes to release of drug in a medium with a certain acidity. In general, SBA-15 brings an inert substrate to loading the drug that can be modified with organic, inorganic materials and polymers to make a smart drug delivery. It can be concluded that SBA-15 is a suitable delivery system for different types of drugs especially in the fields of oral drug delivery. Some disadvantages of SBA-15 delivery systems are their unknown effects on human body, high energy consumption to produce SBA-15 and high-cost surface modification process as well. However, it needs more investigation to compare their advantages and disadvantages.

5. Acknowledgements

We gratefully acknowledge for the financial support from the Research Council of Alzahra University.

6. References

1. N. X. Wang and H. A. von Recum, *Macromol. Biosci.*, 2011, **11**, 321-332.
2. N. Bertrand and J.-C. Leroux, *J. Controlled Release*, 2012, **161**, 152-163.
3. J. S. Beck, J. C. Vartuli, W. J. Roth, M. E. Leonowicz, C. T. Kresge, K. D. Schmitt, C. T. W. Chu, D. H. Olson and E. W. Sheppard, *J. Am. Chem. Soc.*, 1992, **114**, 10834-10843.
4. Q. He and J. Shi, *J. Mater. Chem.*, 2011, **21**, 5845-5855.
5. M. Vallet-Regí, F. Balas and D. Arcos, *Angew. Chem. Int. Ed.*, 2007, **46**, 7548-7558.
6. I. I. Slowing, B. G. Trewyn, S. Giri and V. S. Y. Lin, *Adv. Funct. Mater.*, 2007, **17**, 1225-1236.
7. T. Ukmar and O. Planinšek, *Acta Pharmaceutica*, 2010, **60**, 373-385.
8. S. K. Natarajan and S. Selvaraj, *RSC Adv.*, 2014, **4**, 14328-14334.
9. D. Zhao, J. Feng, Q. Huo, N. Melosh, G. H. Fredrickson, B. F. Chmelka and G. D. Stucky, *Science*, 1998, **279**, 548-552.
10. D. Zhao, Q. Huo, J. Feng, B. F. Chmelka and G. D. Stucky, *J. Am. Chem. Soc.*, 1998, **120**, 6024-6036.
11. G. Mohammadi Ziarani, N. Lashgari and A. Badiei, *J. Mol. Catal. A: Chem.*, 2015, **397**, 166-191.
12. P. Gholamzadeh, G. Mohammadi Ziarani, N. Lashgari, A. Badiei and P. Asadiatouei, *J. Mol. Catal. A: Chem.*, 2014, **391**, 208-222.
13. I. Izquierdo-Barba, M. Colilla, M. Manzano and M. Vallet-Regí, *Microporous Mesoporous Mater.*, 2010, **132**, 442-452.
14. Q. He, J. Zhang, F. Chen, L. Guo, Z. Zhu and J. Shi, *Biomaterials*, 2010, **31**, 7785-7796.
15. T. O. Cheng, *Int. J. Cardiol.*, **121**, 9-22.
16. H. Wang, X. Gao, Y. Wang, J. Wang, X. Niu and X. Deng, *Ceram. Int.*, 2012, **38**, 6931-6935.
17. A. R. Brás, E. G. Merino, P. D. Neves, I. M. Fonseca, M. Dionísio, A. Schönhals and N. T. Correia, *J. Phys. Chem. C*, 2011, **115**, 4616-4623.
18. A. Badiei, I. Haririan, A. Jahangir and G. M. Ziarani, 2009.
19. A. Badiei, Z. Bahrami, A. Jahangir and G. M. Ziarani, *Int. J. Bio-Inorg. Hynrid Nanomater.*, 2014, **3**, 75-80.
20. I. Izquierdo-Barba, E. Sousa, J. C. Doadrio, A. L. Doadrio, J. P. Pariente, A. Martínez, F. Babonneau and M. Vallet-Regí, *J. Sol-Gel Sci. Technol.*, 2009, **50**, 421-429.
21. T. Heikkilä, J. Salonen, J. Tuura, N. Kumar, T. Salmi, D. Y. Murzin, M. S. Hamdy, G. Mul, L. Laitinen, A. M. Kaukonen, J. Hirvonen and V. P. Lehto, *Drug Deliv.*, 2007, **14**, 337-347.
22. S. W. Song, K. Hidajat and S. Kawi, *Langmuir*, 2005, **21**, 9568-9575.
23. K. Lee, D. Lee, H. Lee, C. K. Kim, Z. Wu and K. Lee, *Korean J. Chem. Eng.*, 2010, **27**, 1333-1337.
24. A. Szegedi, M. Popova, I. Goshev and J. Mihály, *J. Solid State Chem.*, 2011, **184**, 1201-1207.
25. L. Gao, J. Sun, L. Zhang, J. Wang and B. Ren, *Mater. Chem. Phys.*, 2012, **135**, 786-797.
26. D. H. Hwang, D. Lee, H. Lee, D. Choe, S. H. Lee and K. Lee, *Korean J. Chem. Eng.*, 2010, **27**, 1087-1092.
27. D. Li, J. Yu and R. Xu, *Chem. Commun.*, 2011, **47**, 11077-11079.

28. F. Rehman, P. L. O. Volpe and C. Airoldi, *Colloids Surf., B*, 2014, **119**, 82-89.
29. B. S. Tian and C. Yang, *J. Nanosci. Nanotechnol.*, 2011, **11**, 1871-1879.
30. T. Higuchi, *J. Pharm. Sci.*, 1963, **52**, 1145-1149.
31. B. González, M. Colilla, C. L. De Laorden and M. Vallet-Regí, *J. Mater. Chem.*, 2009, **19**, 9012-9024.
32. S. Shen, P. S. Chow, F. Chen and R. B. H. Tan, *Chem. Pharm. Bull.*, 2007, **55**, 985-991.
33. V. Cauda, S. Fiorilli, B. Onida, E. Vernè, C. Vitale Brovarone, D. Viterbo, G. Croce, M. Milanesio and E. Garrone, *J. Mater. Sci.: Mater. Med.*, 2008, **19**, 3303-3310.
34. S. Huang, P. Yang, Z. Cheng, C. Li, Y. Fan, D. Kong and J. Lin, *J. Phys. Chem. C*, 2008, **112**, 7130-7137.
35. S. Zhu, Z. Zhou and D. Zhang, *ChemPhysChem*, 2007, **8**, 2478-2483.
36. S. Zhu, Z. Zhou, D. Zhang, C. Jin and Z. Li, *Microporous Mesoporous Mater.*, 2007, **106**, 56-61.
37. H. M. Lin, R. Xing, X. Wu, P. P. Jiang, J. J. Jiang and F. Y. Qu, *Mater. Res. Innovations*, 2013, **17**, 360-365.
38. J. Ma, H. Lin, X. Li, C. Bian, D. Xiang, X. Han, X. Wu and F. Qu, *Mater. Sci. Eng. C.*, 2014, **39**, 21-28.
39. 1967.
40. P. Yang, S. Huang, D. Kong, J. Lin and H. Fu, *Inorg. Chem.*, 2007, **46**, 3203-3211.
41. H. P. Bi, M. Guan, J. C. Li and T. H. Liu, *J. Porous Mater.*, 2013, **20**, 1299-1304.
42. M. Guo, X. Zou, H. Ren, F. Muhammad, C. Huang, S. Qiu and G. Zhu, *Microporous Mesoporous Mater.*, 2011, **142**, 194-201.
43. M. Moritz and M. Łaniecki, *Appl. Surf. Sci.*, 2012, **258**, 7523-7529.
44. F. Richy, O. Bruyere, O. Ethgen, V. Rabenda, G. Bouvenot, M. Audran, G. Herrero-Beaumont, A. Moore, R. Eliakim, M. Haim and J.-Y. Reginster, *Ann. Rheum. Dis.*, 2004, **63**, 759-766.
45. D. Halamová, M. Badaničová, V. Zeleňák, T. Gondová and U. Vainio, *Appl. Surf. Sci.*, 2010, **256**, 6489-6494.
46. S. Huang, C. Li, Z. Cheng, Y. Fan, P. Yang, C. Zhang, K. Yang and J. Lin, *J. Colloid Interface Sci.*, 2012, **376**, 312-321.
47. J. M. Rosenholm and M. Lindén, *J. Controlled Release*, 2008, **128**, 157-164.
48. T. Limnell, T. Heikkilä, H. A. Santos, S. Sistonen, S. Hellstén, T. Laaksonen, L. Peltonen, N. Kumar, D. Y. Murzin, M. Louhi-Kultanen, J. Salonen, J. Hirvonen and V. P. Lehto, *Int. J. Pharm.*, 2011, **416**, 242-251.
49. Y. Wang, Q. Zhao, Y. Hu, L. Sun, L. Bai, T. Jiang and S. Wang, *Int. J. Nanomed.*, 2013, **8**, 4015-4031.
50. M. Moritz and M. Laniecki, *Powder Technol.*, 2012, **230**, 106-111.
51. M. Moritz and M. Łaniecki, *J. Solid State Chem.*, 2011, **184**, 1761-1767.
52. N. Liédana, E. Marín, C. Téllez and J. Coronas, *Chem. Eng. J.*, 2013, **223**, 714-721.
53. Humphries and Merritt, *Aliment. Pharmacol. Ther.*, 1999, **13**, 18-26.
54. Q. Tang, N. Yu, Z. Li, D. Wu and Y. Sun, in *Stud. Surf. Sci. Catal.*, eds. S. Abdelhamid and J. Mietek, Elsevier, 2005, vol. Volume 156, pp. 649-656.
55. W. J. Xu, Q. Gao, Y. Xu, D. Wu and Y. H. Sun, *Acta Chim. Sinica*, 2008, **66**, 1658-1662.
56. P. Agon, P. Goethals, D. Van Haver and J.-M. Kaufman, *J. Pharm. Pharmacol.*, 1991, **43**, 597-600.
57. L. G. R. DeLima, E. D. Kharasch and S. Butler, *Anesthesiology*, 1995, **83**, 204-207.
58. A. De Sousa and E. M. B. De Sousa, *Braz. Arch. Biol. and Technol.*, 2005, **48**, 243-250.
59. Y. Cao, Y.-M. Zhou, Y. Shan, H. Ju and X. Xue, *Chin. Inorg. Chem.*, 2005, **21**, 331-336.
60. L. B. Fagundes, T. G. F. Sousa, A. Sousa, V. V. Silva and E. M. B. Sousa, *J. Non-Cryst. Solids*, 2006, **352**, 3496-3501.

61. K. C. Souza, J. D. Ardisson and E. M. B. Sousa, *J. Mater. Sci.: Mater. Med.*, 2009, **20**, 507-512.
62. A. De Sousa, D. A. Maria, R. G. De Sousa and E. M. B. De Sousa, *J. Mater. Sci.*, 2010, **45**, 1478-1486.
63. A. De Sousa, K. C. De Souza, P. M. Da Silva Leite, R. G. De Sousa and E. M. B. De Sousa, *J. Nanomater.*, 2014, **2014**, 1-10.
64. I. F. Alexa, M. Ignat, R. F. Popovici, D. Timpu and E. Popovici, *Int. J. Pharm.*, 2012, **436**, 111-119.
65. F. Qu, G. Zhu, S. Huang, S. Li, J. Sun, D. Zhang and S. Qiu, *Microporous Mesoporous Mater.*, 2006, **92**, 1-9.
66. R. F. Popovici, E. M. Seftel, G. D. Mihai, E. Popovici and V. A. Voicu, *J. Pharm. Sci.*, 2011, **100**, 704-714.
67. H.-H. Parving, B. M. Brenner, J. J. V. McMurray, D. de Zeeuw, S. M. Haffner, S. D. Solomon, N. Chaturvedi, F. Persson, A. S. Desai, M. Nicolaides, A. Richard, Z. Xiang, P. Brunel and M. A. Pfeffer, *N. Engl. J. Med.*, 2012, **367**, 2204-2213.
68. R. J. Ahern, J. P. Hanrahan, J. M. Tobin, K. B. Ryan and A. M. Crean, *Eur. J. Pharm. Sci.*, 2013, **50**, 400-409.
69. V. Ambrogi, L. Perioli, C. Pagano, F. Marmottini, M. Ricci, A. Sagnella and C. Rossi, *Eur. J. Pharm. Sci.*, 2012, **46**, 43-48.
70. N. Janjua and S. A. Mayer, *Curr. Opin. Crit. Care*, 2003, **9**, 113-119.
71. H. Yu and Q. Z. Zhai, *Microporous Mesoporous Mater.*, 2009, **123**, 298-305.
72. T. Ukmar, G. Mali and O. Planinšek, *Farmacevtski Vestnik*, 2009, **60**, 313-318.
73. R. Mellaerts, J. A. G. Jammaer, M. Van Speybroeck, H. Chen, J. V. Humbeeck, P. Augustijns, G. Van den Mooter and J. A. Martens, *Langmuir*, 2008, **24**, 8651-8659.
74. M. Vialpando, A. Aerts, J. Persoons, J. Martens and G. Van Den Mooter, *J. Pharm. Sci.*, 2011, **100**, 3411-3420.
75. R. Mellaerts, K. Houthoofd, K. Elen, H. Chen, M. Van Speybroeck, J. Van Humbeeck, P. Augustijns, J. Mullens, G. Van den Mooter and J. A. Martens, *Microporous Mesoporous Mater.*, 2010, **130**, 154-161.
76. R. Mellaerts, A. Aerts, T. P. Caremans, J. Vermant, G. Van Den Mooter, J. A. Martens and P. Augustijns, *Mol. Pharm.*, 2010, **7**, 905-913.
77. S. Panage, V. Pande, S. Patil and S. Borbane, *Der Pharmacia Lettre*, 2014, **6**, 159-168.
78. E. I. Basaldella and M. S. Legnoverde, *J. Sol-Gel Sci. Technol.*, 2010, **56**, 191-196.
79. M. S. Legnoverde, I. Jiménez-Morales, A. Jiménez-Morales, E. Rodríguez-Castellón and E. I. Basaldella, *Med. Chem.*, 2013, **9**, 672-680.
80. M. S. Legnoverde, S. Simonetti and E. I. Basaldella, *Appl. Surf. Sci.*, 2014, **300**, 37-42.
81. A. L. Doadrio, E. M. B. Sousa, J. C. Doadrio, J. Pérez Pariente, I. Izquierdo-Barba and M. Vallet-Regí, *J. Controlled Release*, 2004, **97**, 125-132.
82. J. M. Xue and M. Shi, *J. Controlled Release*, 2004, **98**, 209-217.
83. Y. Zhu, S. Kaskel, T. Ikoma and N. Hanagata, *Microporous Mesoporous Mater.*, 2009, **123**, 107-112.
84. M. D. Popova, Á. Szegedi, I. N. Kolev, J. Mihály, B. S. Tzankov, G. T. Momekov, N. G. Lambov and K. P. Yoncheva, *Int. J. Pharm.*, 2012, **436**, 778-785.
85. N. M. Fisher, E. Marsh and R. Lazova, *J. Am. Acad. Dermatol.*, 2014, **49**, 730-732.
86. A. Szegedi, M. Popova, K. Yoncheva, J. Makk, J. Mihaly and P. Shestakova, *J. Mater. Chem. B.*, 2014, **2**, 6283-6292.
87. L. Cui, A. Iwamoto, J.-Q. Lian, H.-m. Neoh, T. Maruyama, Y. Horikawa and K. Hiramatsu, *Antimicrob. Agents Chemother.*, 2006, **50**, 428-438.
88. D. Carmona, F. Balas and J. Santamaria, *Mater. Res. Bull.*, 2014, **59**, 311-322.
89. A. L. Doadrio, J. C. Doadrio, J. M. Sánchez-Montero, A. J. Salinas and M. Vallet-Regí, *Microporous Mesoporous Mater.*, 2010, **132**, 559-566.
90. Q. Yang, S. Wang, P. Fan, L. Wang, Y. Di, K. Lin and F.-S. Xiao, *Chem. Mater.*, 2005, **17**, 5999-6003.

91. V. Cauda, B. Onida, B. Platschek, L. Mühlstein and T. Bein, *J. Mater. Chem.*, 2008, **18**, 5888-5899.
92. D. Molina-Manso, M. Manzano, J. C. Doadrio, G. Del Prado, A. Ortiz-Pérez, M. Vallet-Regí, E. Gómez-Barrena and J. Esteban, *Int. J. Antimicrob. Agents*, 2012, **40**, 252-256.
93. M. Vallet-Regí, J. C. Doadrio, A. L. Doadrio, I. Izquierdo-Barba and J. Pérez-Pariente, *Solid State Ionics*, 2004, **172**, 435-439.
94. F. Sevimli and A. Yilmaz, *Microporous Mesoporous Mater.*, 2012, **158**, 281-291.
95. S. Hashemikia, N. Hemmatinejad, E. Ahmadi and M. Montazer, *J. Colloid Interface Sci.*, 2015, **443**, 105-114.
96. B. Vu, E. Shin, O. Snisarenko, W. Jeong and H. Lee, *Korean J. Chem. Eng.*, 2010, **27**, 116-120.
97. S. K. Das, M. K. Bhunia, D. Chakraborty, A. R. Khuda-Bukhsh and A. Bhaumik, *Chem. Commun.*, 2012, **48**, 2891-2893.
98. J. M. Zuckerman, *Infect. Dis. Clin. N. Am.*, 2004, **18**, 621-649.
99. J. C. Doadrio, E. M. B. Sousa, I. Izquierdo-Barba, A. L. Doadrio, J. Perez-Pariente and M. Vallet-Regí, *J. Mater. Chem.*, 2006, **16**, 462-466.
100. I. Jabbari Zahir Abadi, O. Sadeghi, H. R. Lotfizadeh Zhad, N. Tavassoli, V. Amani and M. M. Amini, *J. Sol-Gel Sci. Technol.*, 2012, **61**, 90-95.
101. I. S. Shin, H. Masuda and K. Naohide, *Int. J. Food Microbiol.*, 2004, **94**, 255-261.
102. S. Y. Park, M. Barton and P. Pendleton, *Colloids Surf., A*, 2011, **385**, 256-261.
103. S. Y. Park and P. Pendleton, *Powder Technol.*, 2012, **223**, 77-82.
104. P. P. Major, A. Lipton, J. Berenson and G. Hortobagyi, *Cancer*, 2000, **88**, 6-14.
105. G. H. Nancollas, R. Tang, R. J. Phipps, Z. Henneman, S. Gulde, W. Wu, A. Mangood, R. G. G. Russell and F. H. Ebetino, *Bone*, 2006, **38**, 617-627.
106. M. Vila, M. Cicuendez, J. Sanchez-Marcos, V. Fal-Miyar, M. Manzano, C. Prieto and M. Vallet-Regi, *J. Biomed. Mater. Res., Part A*, 2013, **101 A**, 213-221.
107. M. Manzano, G. Lamberti, I. Galdi and M. Vallet-Regí, *AAPS PharmSciTech*, 2011, **12**, 1193-1199.
108. M. Colilla, F. Balas, M. Manzano and M. Vallet-Regí, *Chem. Mater.*, 2007, **19**, 3099-3101.
109. M. Colilla, I. Izquierdo-Barba and M. Vallet-Regí, *Microporous Mesoporous Mater.*, 2010, **135**, 51-59.
110. A. Nieto, F. Balas, M. Colilla, M. Manzano and M. Vallet-Regí, *Microporous Mesoporous Mater.*, 2008, **116**, 4-13.
111. P. Jani, G. W. Halbert, J. Langridge and A. T. Florence, *J. Pharm. Pharmacol.*, 1990, **42**, 821-826.
112. J. Juárez, S. G. López, A. Cambón, P. Taboada and V. Mosquera, *J. Phys. Chem., B.*, 2009, **113**, 10521-10529.
113. T. Wang, H. Jiang, Q. Zhao, S. Wang, M. Zou and G. Cheng, *Int. J. Pharm.*, 2012, **436**, 351-358.
114. T. P. B. Nguyen, J. W. Lee, W. G. Shim and H. Moon, *Microporous Mesoporous Mater.*, 2008, **110**, 560-569.
115. S. W. Song, K. Hidajat and S. Kawi, *Chem. Commun.*, 2007, 4396-4398.
116. N. Gargiulo, I. De Santo, F. Causa, D. Caputo and P. A. Netti, *Microporous Mesoporous Mater.*, 2013, **167**, 71-75.
117. K. Motojima, S. Kanaya and S. Goto, *J. Biol. Chem.*, 1988, **263**, 16677-16681.
118. S. Muthukoori, N. Narayanan, M. S. S. Chandra, S. Sethuraman and U. M. Krishnan, *J. Biomed. Nanotechnol.*, 2013, **9**, 907-914.
119. M. E. Revenis and M. A. Kaliner, *J. Pediatr.*, **121**, 262-270.
120. M. S. Bhattacharyya, P. Hiwale, M. Piras, L. Medda, D. Steri, M. Piludu, A. Salis and M. Monduzzi, *J. Phys. Chem. C*, 2010, **114**, 19928-19934.
121. S. I. Kim, T. T. Pham, J. W. Lee and S. H. Roh, *J. Nanosci. Nanotechnol.*, 2010, **10**, 3467-3472.

122. T. Lopez, E. Ortiz, R. Alexander-Katz, E. Basaldella and X. Bokhimi, *Nanomed.: Nanotechnol. Biol. Med.*, 2009, **5**, 170-177.
123. L. Pasqua, L. Veltri, B. Gabriele, F. Testa and G. Salerno, *J. Porous Mater.*, 2013, **20**, 917-925.
124. R. A. García-Muñoz, V. Morales, M. Linares, P. E. González, R. Sanz and D. P. Serrano, *J. Mater. Chem. B.*, 2014, **2**, 7996-8004.
125. P. R. Shorten, C. D. McMahon and T. K. Soboleva, *Biophys. J.*, 2007, **93**, 3001-3007.
126. A. Z. Siavashani, M. H. Nazarpak, F. F. Bakhsh, T. Toliyat and M. Solati-Hashjin, in *Advanced Materials Research*, Trans Tech Publications Inc., Zurich-Durnten, Switzerland, 2014, vol. 829, ch. 4: Nanobiomaterials, pp. 251-257.
127. Q. Jin, F. Qu, J. Jiang, Y. Dong, W. Guo and H. Lin, *J. Sol-Gel Sci. Technol.*, 2013, **66**, 466-471.
128. O. Tacar, P. Sriamornsak and C. R. Dass, *J. Pharm. Pharmacol.*, 2013, **65**, 157-170.
129. C. O. Kim, S. J. Cho and J. W. Park, *J. Colloid Interface Sci.*, 2003, **260**, 374-378.
130. J. Pang, L. Zhao, L. Zhang, Z. Li and Y. Luan, *J. Colloid Interface Sci.*, 2013, **395**, 31-39.
131. Z. Bahrami, A. Badiei and F. Atyabi, *Chem. Eng. Res. Des.*, 2014, **92**, 1296-1303.
132. T. Kjellman, X. Xia, V. Alfredsson and A. E. Garcia-Bennett, *J. Mater. Chem. B.*, 2014, **2**, 5265-5271.
133. M. Vafaee, M. M. Amini, E. Najafi, O. Sadeghi and V. Amani, *J. Sol-Gel Sci. Technol.*, 2012, **64**, 411-417.
134. R. Vathyam, E. Wondimu, S. Das, C. Zhang, S. Hayes, Z. Tao and T. Asefa, *J. Phys. Chem. C*, 2011, **115**, 13135-13150.
135. I. F. Alexa, C. G. Pastravanu, M. Ignat and E. Popovici, *Colloids Surf., B*, 2013, **106**, 135-139.
136. K. S. Elmslie and D. Yoshikami, *Brain Res.*, 1985, **330**, 265-272.
137. T. López, E. Ortiz, E. Gómez, V. P. D. L. Cruz, P. Carrillo-Mora and O. Novaro, *J. Nanomater.*, 2014, **2014**.
138. Z. Wang, B. Chen, G. Quan, F. Li, Q. Wu, L. Dian, Y. Dong, G. Li and C. Wu, *Int. J. Nanomed.*, 2012, **7**, 5807-5818.
139. L. Činčárová, Z. Zdráhal and J. Fajkus, *Expert Opin. Invest. Drugs*, 2013, **22**, 1535-1547.
140. M. A. Rogawski and W. Loscher, *Nat. Rev. Neurosci.*, 2004, **5**, 553-564.
141. T. López, E. I. Basaldella, M. L. Ojeda, J. Manjarrez and R. Alexander-Katz, *Opt. Mater.*, 2006, **29**, 75-81.

Authors' Biographies

Ghodsi Mohammadi Ziarani was born in Iran, in 1964. She received her B.Sc. degree in Chemistry from the Teacher Training University, Tehran, Iran, in 1987, her M.Sc. degree in Organic Chemistry from the same university, under the supervision of Professor Jafar Asgarin and Professor Mohammad Ali Bigdeli in 1991. She obtained her Ph.D. degree in asymmetric synthesis (Biotransformation) from Laval University, Quebec, Canada under the supervision of Professor Chenevert, in 2000. She is an Full Professor in the Science faculty of Alzahra University. Her research interests include organic synthesis, heterocyclic synthesis, asymmetric synthesis, natural products synthesis, synthetic methodology and applications of nano-heterogeneous catalysts in multicomponent reactions.

Alireza Badiei was born in Iran, in 1965. He received B.Sc. and M.Sc. degrees in Chemistry and Inorganic Chemistry from the Teacher Training University (Kharazmi),

Tehran, Iran, in 1988 and 1991, respectively, and his Ph.D. degree in Synthesis and Modification of Nanoporous Materials from Laval University, Quebec, Canada, in 2000. He is currently Full Professor in the Chemistry Faculty of Tehran University. His research interests include nanoporous materials synthesis, modification of nanoporous materials and application of organic–inorganic hybrid materials in various fields such as catalysis, adsorption, separation and sensors.

Vaezeh Fathi Vavsari was born in 1983 in Sari, Iran. She received her B.Sc. degree in Applied Chemistry from Ferdowsi University of Mashhad, Iran (2009) and her M.Sc. degree in Organic Chemistry at Khaje Nasir Toosi University of Technology, Tehran, Iran (2013) under the supervision of Dr. Saeed Balalaie. She is currently working towards her Ph.D. in Organic chemistry at Alzahra University under the supervision of Dr. Ghodsi Mohammadi Ziarani. Her research field is organic synthesis by the using of amino acids and hydrazides in the presence of nanostructure silicas as catalysts.